

RECEIVED: February 27, 2022 ACCEPTED: June 27, 2022 PUBLISHED: August 18, 2022

6D anomaly-free matter spectrum in F-theory on singular spaces

Antonella Grassi, a,d James Halverson, b,f Cody Long, c Julius L. Shaneson, d Benjamin Sung b and Jiahua Tian e

- ^a Dipartimento di Matematica, Università di Bologna, Bologna 40126, Italy
- ^bDepartment of Physics, Northeastern University, Boston, MA 02115, U.S.A.
- ^c Jefferson Physical Laboratory, Harvard University, Cambridge, MA 02138, U.S.A.
- ^dDepartment of Mathematics, University of Pennsylvania, Philadelphia, PA 19104, U.S.A.
- ^e Abdus Salam International Centre for Theoretical Physics, Str. Costiera, 11, Trieste 34151, Italy
- f The NSF AI Institute for Artificial Intelligence and Fundamental Interactions
 E-mail: grassi@math.upenn.edu, j.halverson@northeastern.edu,
 clong@g.harvard.edu, shaneson@math.upenn.edu,
 sung.b@northeastern.edu, jtian@ictp.it

ABSTRACT: In this paper we study the 6d localized charged matter spectrum of F-theory directly on a singular elliptic Calabi-Yau 3-fold, i.e. without smoothing via resolution or deformation of the entire fibration. Given only the base surface, discriminant locus, and the $SL(2,\mathbb{Z})$ local system, we propose a general prescription for determining the charged matter spectrum localized at intersections of seven-branes, using the technology of string junctions. More precisely, at each codimension-2 collision of seven-branes, we determine the local seven-brane content and compute the number of massless string junctions modulo the action of the $SL(2,\mathbb{Z})$ monodromy. We find agreement with the predicted results from 6d anomaly cancellation in all cases considered. Examples include a generic Weierstrass model with arbitrary Kodaira fiber intersecting an I_1 , as well as cases with jointly charged matter localized at intersections of non-abelian seven-branes.

Keywords: Anomalies in Field and String Theories, F-Theory

ARXIV EPRINT: 2110.06943

\mathbf{C}	ontents	
1	Introduction	1
2	Vanishing cycles and minimal normal factorizations	\$
3	Matter in 6D F-theory compactifications on singular spaces	Ę
4	Examples: matter on singular spaces and anomaly cancellation	11
	4.1 Type $I_n, n \geq 2$	13
	4.1.1 Matter in n	1:
	4.1.2 Matter in Λ^2	13
	4.2 Type I_n^*	18
	4.3 Type III	20
	4.4 Type IV_s	20
	4.5 Type IV_s^*	25
	4.6 Type III^*	26
	$4.7 III \times III$	2'
	$4.8 IV_s \times IV_s$	28
	$4.9 IV_s \times III$	29
5	Remarks on localized neutral hypermultiplets	31

1 Introduction

F-theory [1, 2] is a non-perturbative formulation of type IIB superstring theory that geometrizes seven-brane physics. Specifically, the axio-dilaton profile sourced by the seven-branes is encoded in an elliptically fibered Calabi-Yau variety $X \to B$. The singularities of X encode the structure of seven-branes, providing the geometric and topological data that is crucial for determining the degrees of freedom of the F-theory compactification and their low-energy physics. Though unbroken non-abelian gauge symmetry on seven-branes requires singularities in the F-theory description, many analyses nevertheless smooth the variety. For instance, a series of blowups and small resolutions [3–11] may yield a smooth Calabi-Yau fourfold X^{\sharp} , where M-theory on X^{\sharp} corresponds to the Coulomb branch of an associated 3d $\mathcal{N}=2$ theory, obtained by compactification of the 4d theory on a circle. Another approach is to obtain a smooth Calabi-Yau fourfold X^{\flat} by a complex structure deformation [12–21], which corresponds to a Higgsing of the 4d $\mathcal{N}=1$ gauge group associated to the 7-branes. Both techniques are indirect, however, as the smoothing moves the theory to a different phase. There is no guarantee that the physics of F-theory on X is completely captured by the geometry and topology of X^{\sharp} or X^{\flat} .

Instead, to understand compactifications with unbroken seven-brane gauge symmetry it is preferable to study that phase directly, i.e. via the singular geometry and topology of X itself. Doing so requires the development of new mathematics, such as in the study of F-theory on singular spaces via matrix factorizations [22] or via string junctions [23]; the latter built on a mathematical theory of topological string junctions [20] developed in the case of a smooth variety.

In this work we continue to develop a theory of F-theory on singular spaces that utilizes string junctions. Indeed, our approach emphasizes the definition of F-theory as $SL(2,\mathbb{Z})$ -equivariant type IIB supergravity coupled with background (p,q) 7-branes. From this perspective, the background spacetime is smooth and it is natural to establish an algorithm that generalizes the original counting of localized charged and uncharged matter at the intersections of D7-branes in terms of open string states. String junctions thus serve as a natural tool, and our proposal reduces precisely to the original counting in the case that all (p,q) 7-branes are mutually local, i.e. in the weakly coupled type IIB limit.

Specifically, we give a description of computing the localized charged matter spectrum at the intersection of two irreducible components of the discriminant locus. The main results of the paper are as follows, organized according to the section in which they appear. In section 3:

- Given a discriminant of the form $\Delta = z^n \tilde{\Delta}$, we obtain sets S_G , S_R of vanishing cycles corresponding to the seven-brane content obtained from the local monodromy around $z^n = 0$, and also from the local monodromy around $\tilde{\Delta} = 0$ restricted to the plane $z = \epsilon$. We count the number of root junctions associated to the sets S_G and S_R , using methods from [23].
- The threefold geometry induces a monodromy on the junctions that is crucial to compute the charged matter spectrum and match what is known from anomaly cancellation. Specifically, we compute the monodromy matrices $M_G M_R$, $M_G M_R^{-1}$ and their inverses, and identify asymptotic charges (and therefore junctions with those charges) that are related by monodromies generated from this set.
- We argue that these monodromies coincide with a representation of the fundamental group of the complement of \mathbb{C}^2 by the union of two lines through the origin, and argue that this coincides with the physics via a Higgsing.
- In the cases with matter charged under a product gauge group $G \times G'$, we use the same prescription by choosing S_G, M_G from the set of seven-branes forming one gauge group factor G, and the residual data S_R, M_R from G' together with the other residual seven-branes.

We study many examples in section 4. Specifically:

- We verify the above prescription in all cases with a generic tuning of a single Kodaira fiber intersecting with a residual I_1 , assuming normal crossing.
- We verify the above prescription for cases with jointly charged matter for $III \times III, IV_s \times IV_s$, and $IV_s \times III$, again assuming normal crossing.

A subtlety regarding localized neutral hypermultiplets is studied in section 5. Specifically,

• We exhibit an example of tunings of $III-I_1$ which yields the same number of localized charged hypermultiplets but different localized neutrals depending on the tuning. In particular, our entire prescription is completely independent of details of the tuning. A specific example is given at the end of the section.

2 Vanishing cycles and minimal normal factorizations

Consider an elliptic fibration $\pi: X \to B$ over a complex algebraic surface B described by a Weierstrass model

$$y^2 = x^3 + fx + g\,, (2.1)$$

where $f \in \mathcal{O}(-4K_B)$, $g \in \mathcal{O}(-6K_B)$. The fiber degenerates along the discriminant locus $D \subset B$

$$D := \{ \Delta = 4f^3 + 27g^2 = 0 \}, \qquad (2.2)$$

which is the location of the seven-branes.

Smooth case

For the sake of simplifying the discusion, we first assume that the total space X is non-singular and that all vanishing cycles are simple (p,q)-cycles, i.e., the vanishing cycle is pa + qb where a and b are the meridian and longitudinal cycles of the elliptic curve E, respectively. We will refer to this as a simple type degeneration, where all codimension-one singularities are of type I_1 . The $SL(2, \mathbf{Z})$ monodromy matrix associated with looping around a component of D takes the form

$$M_{(p,q)} = \begin{pmatrix} 1 - pq & p^2 \\ -q^2 & 1 + pq \end{pmatrix}. \tag{2.3}$$

In this work the correspondence between the geometry of the elliptic curve E and its $SL(2,\mathbb{Z})$ representation, or the correspondence between geometric data and algebraic data, will play a crucial role. The geometric data can be read off by studying the motion of the three roots of the equation

$$x^3 + fx + g = 0, (2.4)$$

as one completes a closed path encircling a component $D_i \subset D$. At a generic point p away from D the three roots are distinct, and we can choose a labeling of these roots x_1, x_2, x_3 , which provides a canonical definition of the cycles $\pi_1 := (1,0), \pi_2 := (-1,-1)$ and $\pi_3 := (0,1)$ given such a labeling. In figure 1 we plot the roots in the x-plane, as well as the cycles. Such a choice is made up to a global SL(2, Z) transformation. These labels denote the vanishing cycles as two roots collide along components of D.

The cycles π_1 , π_2 and π_3 are a (over-complete) set of generators of $H_1(E,\mathbb{Z})$, where E is the fiber at p. Fixing a reference point p away from D, as we approach D a (p,q)-cycle vanishes, as we are only considering degenerations of a simple type, i.e., we are considering smooth X with only I_1 fibers. For instance, if a (1,0)-cycle vanishes, x_1 and x_3 approach each other and become degenerate on D. To properly analyze the monodromy, one should

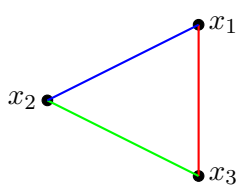


Figure 1. The three solutions x_1, x_2, x_3 to $x^3 + fx + g = 0$ are plotted at a generic smooth point. We define the cycles π_i such that the red line segment denotes π_1 , the green line segment denotes π_2 and the blue line segment denotes π_3 .

then perform a loop around D; for instance, taking a loop around D, for which the vanishing cycle is (1,0), will induce a geometric swap of the roots x_1 and x_3 .

Singular case. However, the case that the total space X is singular is both more physically interesting, and more generic, and we can no longer restrict ourselves to simple type degenerations. When approaching D, x_1 , x_2 and x_3 will usually all degenerate into one point. In such cases one needs further tools to analyze the vanishing cycles and monodromy. As discussed in the Introduction, this may be done either via resolution or deformation, but both methods are indirect (likely losing information of the unbroken phase), and we prefer to work directly with the singular space. Furthermore, in nearly all known cases (e.g. [24, 25]) a smoothing complex structure deformation does not exist. Similarly, some singularities that give rise to localized neutral hypermultiplets cannot be resolved [26].

When X is singular, D is in general a non-reduced scheme, where each component's multiplicity corresponds to the number of (p,q) 7-branes along that component. In this case one cannot read off the vanishing cycles by approaching the components D_i of D (from an appropriately chosen fixed point), but instead must infer a set of vanishing cycles via the motion of the roots induced by traversing a loop around each D_i . While the motion of the roots is in general not a simple exchange (except in the simple I_1 case), any motion can be decomposed into an ordered set of exchanges. Such an ordered set can be used to define a set of vanishing cycles. This choice corresponds to a decomposition of the monodromy matrix M into a minimal normal factorization (MNF), defined in [27]. An MNF of a monodromy matrix is a decomposition of an $SL(2, \mathbb{Z})$ monodromy matrix associated with a Kodaira fiber type into n factors with each factor given by one of the following matrices corresponding to the monodromy sourced by a (1,0) and a (0,1) seven-brane respectively.

$$M_{(1,0)} = \begin{pmatrix} 1 & 1 \\ 0 & 1 \end{pmatrix}, \qquad M_{(0,1)} = \begin{pmatrix} 1 & 0 \\ -1 & 1 \end{pmatrix}$$

Such a factorization exists for each $SL(2,\mathbb{Z})$ -matrix corresponding to a Kodaira fiber and is unique up to Hurwitz moves and we refer to ([23], section 3.2) for an in-depth summary of the results of [27] and its implications for singular string junctions. A Hurwitz move is given by one of the following transformations for $g_i \in G$ (for our purpose, $G = SL(2,\mathbb{Z})$)

$$g_1g_2\cdots g_ig_{i+1}\cdots g_k \to g_1g_2\cdots g_{i+1}(g_{i+1}^{-1}g_ig_{i+1})\cdots g_k$$

or

$$g_1g_2\cdots g_ig_{i+1}\cdots g_k \to g_1g_2\cdots (g_ig_{i+1}g_i^{-1})g_i\cdots g_k,$$

i.e., g_{i+1} is "pulled past" g_i , conjugating it in the process, or vice versa.

Given a disc $C \subset B$ intersecting components of the discriminant locus, we may consider the restriction to an elliptic surface $X_1 \to C$. In the following, we will use the technology of string junctions assuming that they exist as a basis of $H_2(\tilde{X}_1, E_p)$ where \tilde{X}_1 is the total space of a deformation of $X_1 \to C$ to an elliptic surface with only I_1 singularities. We will use a canonical ordering of the vanishing cycles (MNF) given in table 1 and the associated intersection pairing, but the results will be independent of the choice of basis. Despite such assumptions, we emphasize that all these properties of string junctions can be obtained completely algebraically independent of the deformation and in [28], we will demonstrate that all the relevant data such as the intersection pairing are indeed invariant under Hurwitz moves.

3 Matter in 6D F-theory compactifications on singular spaces

Given a Weierstrass or Tate model of an elliptically fibered Calabi-Yau threefold with a gauge group supported on a divisor $D_z := \{z = 0\}$ with z a local coordinate on B, the discriminant locus takes the form

$$\Delta = z^n \tilde{\Delta} \,, \tag{3.1}$$

where $\tilde{\Delta}$ is the residual discriminant locus. Generally there are matter hypermultiplets localized at intersection points $z = \tilde{\Delta} = 0$, and the goal of this work is to count such hypermultiplets. At the intersection the fiber degenerates further, and the gauge algebra is enhanced to a larger one. To study the spectrum at the enhancement point we will probe the point with a D3-brane probe.

As discussed in the previous section we can associate to D_z and (each component of) $\tilde{\Delta}$ an ordered set of vanishing cycles via an MNF. At the collision point the vanishing cycles intersect, and massless matter can be realized by closed string junctions with one boundary supported on D_z , and one boundary supported on $\tilde{\Delta}$. A direct counting of these string junction states supported at the codimension-two locus generally gives a matter spectrum that is too large to satisfy anomaly cancellation. However, we will propose that these states, labeled by their asymptotic charges with respect to D_z , are not all independent, and are related by a set of monodromy actions that identifies some states with one another. To see this, we will focus on a local intersection point of D_z and $\tilde{\Delta}$, which we label u, and probe the enhancement point with a mobile D3 brane. The D3 brane can traverse loops in $B \setminus D$, which will induce an action on the string junctions extending from D_z , to be attached to $\tilde{\Delta}$. The relevant monodromies will be those associated to the point of enhancement, in the following way: fix a point p in a local neighborhood of u. Let us for now assume that D_z and $\tilde{\Delta}$ are locally normal crossing schemes, not necessarily reduced, and let the monodromy matrices M_G and M_R correspond to the monodromy action around D_z and

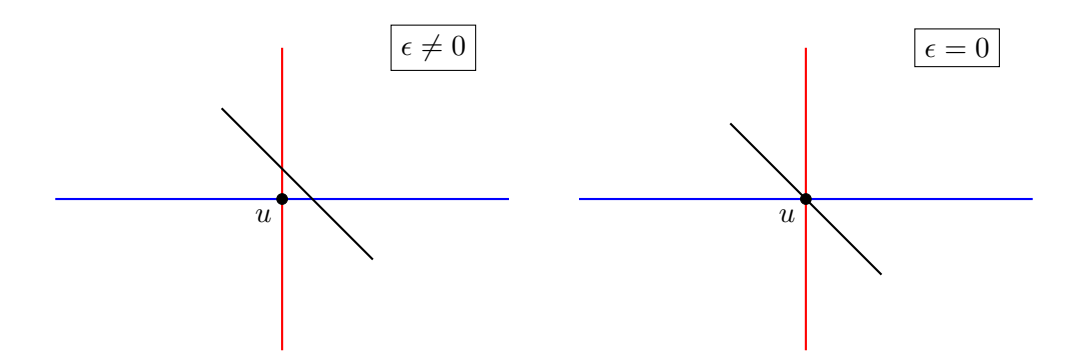


Figure 2. The gauge 7-branes are on top of each other and denoted by the blue line. The residual discriminant locus is denoted by the red line, which for the moment we assume to be normal crossing. The black line segment denotes a disk that intersects the 7-branes. In the left figure the disc misses the codimension-two point u, but intersects the codimension-one loci each at a point. In the right figure the disc has been deformed to intersect u at a point.

 $\tilde{\Delta}$ respectively (G is for gauge and R is for residual). We can then associate with u the monodromy matrices $M_R \cdot M_G$, $M_G \cdot M_R$, $M_R \cdot M_G^{-1}$, $M_R^{-1} \cdot M_G$, and their inverses. Let us call this set of matrices $\{M_u^i\}$, i=1...8.

These matrices have a clear geometric interpretation, realized by a D3 probe approaching u. In order to probe u, we want to study the monodromy associated with u, and since u is associated to the collision of two co-dimension one loci, we can naturally associate the above matrices as u-point monodromies. Let us consider a point p near u on a disk that intersects both z=0 and $\tilde{\Delta}=0$, such that the distance on the disc between z=0 and $\tilde{\Delta}=0$ is a small parameter ϵ . For such a disc one can take the limit $\epsilon \to 0$, such that the only singularity on the disc is the codimension-two point u. This is shown in figure 2. On the disk the geometry is sketched in figure 3. Clearly there are two generators of $\pi_1(B\backslash\Delta)$ on the disc, and the corresponding loops are L_G and L_R , with corresponding monodromy matrices M_G and M_R . Taking the parameter $\epsilon \to 0$, we place the disc so that it only contains the point u as a component of the discriminant Δ . By taking the associated loops in the disc around u we can probe the matter locus via monodromy. On such a disc it is clear there are two loops that can be deformed to encircle u without coming into contact with the discriminant locus. These are $L = L_R \circ L_G$ and $L^{-1} = L_G^{-1} \circ L_R^{-1}$, with associated monodromy matrices $M = M_R \circ M_G$ and $M^{-1} = M_G^{-1} \circ M_R^{-1}$, respectively.

We require that the matter states supported at u are given by the junctions that are invariant under both M and M^{-1} . These monodromies can be read off by studying the motion of the three roots x_1, x_2, x_3 of $y^2 = x^3 + fx + g = 0$ upon traversing the loops L or L^{-1} as in [21, 23]. The geometric motion of the roots can then be associated with an $SL(2,\mathbb{Z})$ monodromy matrix that acts explicitly on the asymptotic charge a(J) of a string junction. More precisely, the connecting homomorphisms

$$\partial: H_2(X_1, E_p) \to H_1(E_p) \tag{3.2}$$

¹Distinguishing between a parameter distance and a proper distance will not be important here as all our studies occur at finite distances in moduli space.

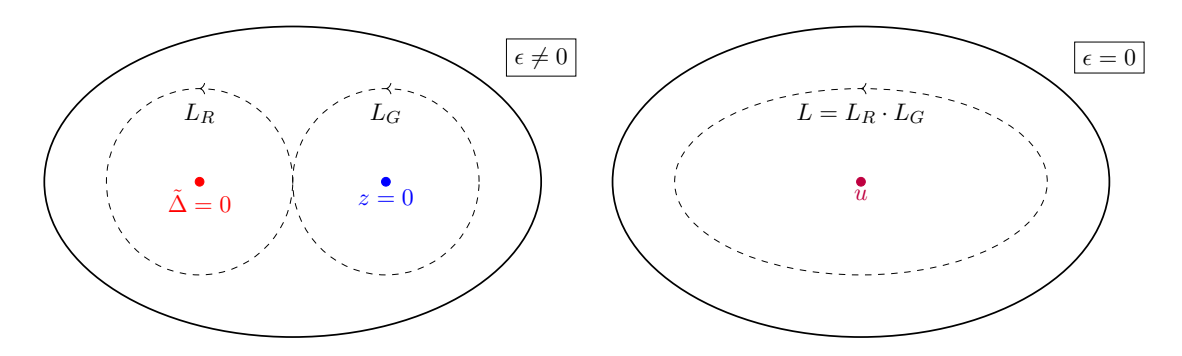


Figure 3. On the disk D near $z = \tilde{\Delta} = 0$ the D3 probe can either traverse the loop $L = L_R \circ L_G$ or the loop $L^{-1} = L_G^{-1} \circ L_R^{-1}$. L_G and L_R are as directed by the arrows. This disc can be deformed to only contain the codimension-two point u, by taking $\epsilon \to 0$.

carries a monodromy on the junctions to the monodromy on the asymptotic charges, where X_1 is the restriction to D of a deformation of $\pi: X \to B$ to a fibration that has only I_1 -singularities when restricted to the intersection of B with all but a finite set of parallel hyperplanes. We assume that, on D, at z=0 there is a stack of gauge 7-branes $S_G=\{\pi_1,\ldots,\pi_i\}$ and $\tilde{\Delta}=0$ consists of 7-branes $S_R=\{\pi_{i+1},\ldots,\pi_n\}$. Naively the matters corresponding to the string junctions J_{GR} stretch between S_G and S_R and can be obtained using the technique developed in [17]. When the brane content S_G+S_R is associated with a gauge algebra these junctions are simply given by the branching rule $G_{S_G+S_R} \to G_{S_G}$ where G_S is the gauge algebra corresponding to the set S of 7-branes. The junctions J_{GR} typically give rise to more matters than are required by 6D anomaly cancellation. The monodromies M and M^{-1} map different junctions with different a(J)'s to each other and this reduction leads to the correct 6D matter spectrum.

The physical interpretation is as follows: a massless state in a representation \mathcal{R} under the gauge group G corresponds to a string junction J supported at u, with non-trivial asymptotic charge a(J) on D_z . Such a junction pinches off on D_z , and also on $\tilde{\Delta}$, with the same asymptotic charge flowing into $\tilde{\Delta}$. We place a D3 probe on this junction, so that the matter state supported at u can be broken into two junctions: a junction J_G with one boundary on the D3 brane and the other on D_z , with asymptotic charge a(J), and a junction J_R with one boundary on the D3 brane and the other on $\tilde{\Delta}$, with asymptotic charge -a(J), such that the junctions can join together to reproduce the full 7-7 junction, see figure 4. To probe these states we arrange for a disc \mathcal{D} containing the point u as the only point of $\Delta \cap D$, and then allow the D3 brane to loop around u. This will induce an action on the asymptotic charge of both J_G and J_R , in a manner such that they can again be joined to create a junction corresponding to charged matter in \mathcal{R} of G. The identification of such states will be necessary to produce the correct amount of charged matter to satisfy 6d anomaly cancellation.

As is clear from both the geometry and the pictures, the disc \mathcal{D} is not unique. We require the disc, at $\epsilon \neq 0$, to intersect both D_z and $\tilde{\Delta}$ at a point, and that these points collide as $\epsilon \to 0$. In fact, there are four such discs that locally achieve this, which correspond to the four quadrants in figure 2. Therefore, for each quadrant we can define the monodromy

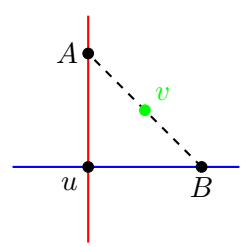


Figure 4. The D3 brane at v denoted by the green dot is placed on the 7-7 junction AB stretched between two stacks of 7-branes intersecting at u. The 7-7 junction is represented by the dashed line and the two stacks of 7-branes are represented by the red and blue lines. The two 3-7 junctions are Av and vB with asymptotic charges a(J) and -a(J) respectively and clearly they combine into the full 7-7 junction AB.

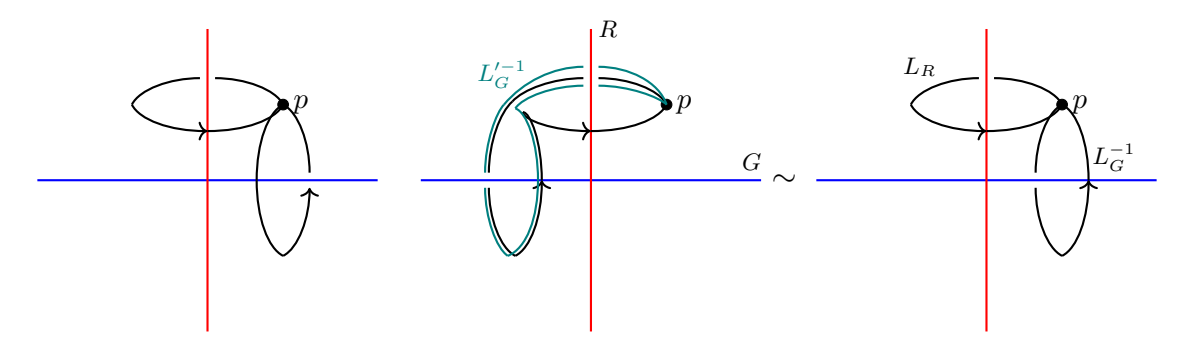


Figure 5. Left two paths denote the possible paths of a D3 probe confined to a disk encircling the intersection of the two 7-brane stacks. The homotopy relation between the right two paths allows one to conclude the monodromy acting on the homology of the elliptic fiber.

matrices M and M^{-1} . Via the fact

$$M_L = M_{L_2} \circ M_{L_1}, \text{ if } L = L_2 \circ L_1,$$
 (3.3)

we have the total set of monodromy matrices associated to u: $M_R \cdot M_G$, $M_G \cdot M_R$, $M_R \cdot M_G^{-1}$, $M_R^{-1} \cdot M_G$, and their inverses which we above labeled $\{M_u^i\}$, $i = 1 \dots 8$. By requiring the matter spectrum be invariant under all $\{M_u^i\}$, we will find the correct amount of matter to satisfy 6d anomaly cancellation. We note that often many of these matrices will induce redundant identifications, and so in the examples we will only note the minimal set of non-trivial ones.

In the above discussion, we have associated natural monodromy matrices to distinguished paths encircling the codimension 2 point given by the two paths on the left of figure 5. We now verify that the above assignments are in fact the correct monodromies realized by the desired paths. In particular, it will suffice to demonstrate that the second path $L_G^{'-1} \circ L_R$ in figure 5 is homotopy equivalent to the third path $L_G^{-1} \circ L_R$, or equivalently that $L_G^{'-1} \sim L_G^{-1}$. Under this assumption, the corresponding $SL(2,\mathbb{Z})$ monodromy representations are equivalent, and hence, all possible codimension 2 monodromies are generated by $M_G \cdot M_R$ and $M_G^{-1} \cdot M_R$.

To see the above homotopy, we will follow the discussion in ([29], section 6.3). Denoting the axes by G and R, the path L_G is given by the circle in the plane $G = G_0$, L_R by the circle in the plane $R = R_0$, and p by the coordinates (1,1). Consider the point x(t) on the circle $R = R_0$ given by $(e^{it},1)$. The homotopy is given at each time t by the path which begins at p, traverses to x(t) along $R = R_0$, goes along the circle (e^{it}, e^{is}) for fixed t, and then goes back to p. This induces the relation $L_G^{-1} \sim L_G'^{-1} \sim L_R \circ L_G^{-1} \circ L_R^{-1}$ and we conclude. In general, we note that the fundamental group of the complement of two normal crossing divisors in an open affine patch is the free abelian group of rank two, i.e. $\pi_1(\mathbb{C}^2 \setminus \{xy = 0\}, p) \cong \mathbb{Z}^2$.

So far we have assumed that the loci $\tilde{\Delta}$ and D_z are normal crossing, in which case near u it is clear that a disc \mathcal{D} intersecting D_z and $\tilde{\Delta}$ will capture all vanishing cycles at u. For general intersections between gauge group divisors and I_1 -loci, this assumption will not be valid; for instance, in the type III- I_1 collision, the discriminant takes the form $\Delta = z^3(27z + 4t^3)$, where at $u = \{z = 0 \cap t = 0\}$, there is a multiplicity-three intersection in t, but away from $\{z = 0\}$ the I_1 locus splits into three components. In this case and similar ones, we must ensure that the $\epsilon \neq 0$ disc is large enough to intersect all components of the I_1 locus near u. Note that while $\tilde{\Delta}$ is in general one large connected subvariety, near u it looks like three separate components, which intersect with multiplicity three at u, and we make \mathcal{D} large enough to capture the three components, and thus the multiplicity three intersection as $\epsilon \to 0$.

We also note that, while the construction of the appropriate discs \mathcal{D} is still achievable, one can instead (locally) start with a simpler model that is locally a normal crossing intersection, and then deform to the model of interest. Such a process corresponds to a Higgsing of a product gauge group $G' \times G \to G$, where G is the gauge group that we want to study. For example, in the $III - I_1$ case, we have

$$f = zF, \ g = z^2G, \ \Delta = z^3(4F^3 + 27G^2z)$$
 (3.4)

for a local coordinate z. Taking another local coordinate $F \sim t$, we have matter localized at t = z = 0. This is clearly not a normal crossing locus, but we can make it so, by taking G = G't, yielding

$$f = ztF', \ g = z^2t^2G', \ \Delta = z^3t^3(4(F')^3 + 27(G')^2),$$
 (3.5)

which is locally normal crossing, and corresponds to a III-III intersection. From this normal crossing model we can arrange the appropriate disc near u, and then deform the geometry an infinitesimal amount to the geometry of interest.

The Higgsing described in the above paragraph then motivates the question: how does this prescription address the counting of localized massless matter for Weierstrass models with states charged under product representations $\mathcal{R}' \oplus \mathcal{R}$? Indeed, the obvious ambiguities in the naive extension of the aforementioned prescription to the case of intersections of multiple non-abelian 7-brane loci are what should we take J_G to be and what is the corresponding codimension-2 monodromy. From the perspective of the above, there are also natural deformations to multiple distinct normal crossing loci.

In general, to count massless matter charged under the representation (\mathbf{m}, \mathbf{n}) of the gauge group $G' \times G$, our prescription will be as follows. Without loss of generality, assume that the representation \mathbf{n} of G is not the trivial representation. We then choose a minimal deformation to a local normal crossing model $H \times G$ where H corresponds to the 7-brane content of G' and any residual 7-brane loci transverse to that of G. Such a deformation corresponds to a natural set of seven-branes $S = S_G \cup S_H$ and the gauge seven-branes within S_H induces an additional partition $S_H = S_{G'} \cup S_R$. Given such partitions, a massless state in the representation (\mathbf{m}, \mathbf{n}) then corresponds to a junction J supported on S and the prescription proceeds exactly as in the above with J_G the sub-junction supported on S_G and codimension-2 monodromy determined by the normal crossing model. In particular, if both factors in the product representation are non-trivial, this determines distinct deformations which yield the same counting of massless matter.

We will illustrate the natural extension of our prescription for the $IV_s - III$ case, which exhibits an unusual feature: a forced codimension-2 collision of three 7-branes, a phenomenon classified in [30]. In this example, we have the assignments

$$f = zt^2, \ g = z^2t^2, \ \Delta = z^3t^4(4t^2 + 27z)$$
 (3.6)

for z and t local coordinates. In particular, there is an additional I_1 loci given by the residual discriminant intersecting the $SU(3) \times SU(2)$ point which is characteristic of this model. For each product representation of $SU(3) \times SU(2)$, we will deform to a local normal crossing model in the spirit of the above example. For massless matter charged under the representation (\mathbf{m}, \mathbf{n}) of $SU(3) \times SU(2)$ with \mathbf{m} non-trivial, we will look at the t-slice and for \mathbf{n} non-trivial, we will look at the z-slice. For each slice, there is a corresponding 7-brane stack, a partition into two sets of gauge seven-branes and residual seven-branes, and a monodromy action.

Concretely, to compute the spectrum of massless matter charged under $(\mathbf{3},\mathbf{1})$, we consider the set of all junctions with support on the set of seven-branes obtained by setting $t = \epsilon$. Given the partition of seven-branes $S_t = \{S_{IV_s} \mid S_{III} \mid I_1\}$, we determine the junctions J charged under the $\mathbf{3}$ of SU(3) given by the gauge branes S_{IV_s} and uncharged under the gauge branes S_{III} . We then compute the monodromy orbit of the asymptotic charge $a(J_{S_{IV_s}})$ under the codimension-2 monodromy determined by S_t and identify the corresponding junctions. Likewise, we carry out a similar procedure for $(\mathbf{1},\mathbf{2})$ by setting $z = \epsilon$ and looking at the brane system $S_z = \{S_{IV_s} \mid S_{III} \mid I_1 \mid I_1\}$ and for the bi-fundamental representation $(\mathbf{3},\mathbf{2})$, both models yield identical results. This computation is detailed in section 4.9.

For most examples the monodromy action described thus far will be enough to reduce the spectrum to that required by anomaly cancellation. In fact, this works precisely when the to-be-identified charged matter states have different asymptotic charges, as the identification is done on the level of asymptotic charge. However, in the case where the over-counting is due to states with the same asymptotic charge there will be a further reduction. Consider a closed string J that encircles u, such that a(J) is an eigenvector of the $\{M_u^i\}$, with eigenvalue one. The lift of this closed string to X_1 is a cylinder with asymptotic charge a(J) = 0, and hence is an element in $H_2(X_1, \mathbb{Z})$. Since the monodromy matrices of

u act trivially on the junction, via a Hanany-Witten move one can pass the closed string directly through u, without the junction gaining prongs localized at u. In a local neighborhood of u, such a junction may appear non-trivial, as it can attach simultaneously to $\tilde{\Delta}$ and D_z , but upon taking the junction to u, where the candidate state would become massless, it becomes trivial, and therefore does not contribute to the matter spectrum. In terms of the monodromy matrices, the condition for such a state to be trivial is

$$(M_u^i - 1) \cdot a(J) = 0, (3.7)$$

for all i. We will refer to such states as HW-trivial. We will find that the combination of the two monodromy actions, from the u-monodromy and the HW-triviality reduction, will reproduce the correct matter spectrum to satisfy anomaly cancellation.

Finally, we remark that our identification of junctions proceeds purely at the level of the asymptotic charges. Such an identification may or may not descend to an identification of the junctions themselves, and we will explore this in future work.

We will use the following notation throughout:

$$\pi_1 := (1,0), \ \pi_2 := (-1,-1), \ \pi_3 := (0,1), \ \pi_\alpha := (1,-1), \ \pi_\beta := (2,1).$$
 (3.8)

We will see the last two appear in the type I_n fiber enhancement.

4 Examples: matter on singular spaces and anomaly cancellation

Having introduced a formalism for counting charged hypermultiplets in 6d F-theory compactifications on singular spaces, including a monodromy quotient necessary for obtaining the correct spectrum, we now apply it in many examples. We find that the matter spectra that we directly compute matches expectations from anomaly cancellation [5, 31, 32].

The data of all of the examples we will discuss in this section are summarized in table 1.

4.1 Type $I_n, n \ge 2$

For type I_n fiber, using a Tate model we have:

$$\Delta = z^n (a_{10}^4 P + \mathcal{O}(z)) \tag{4.1}$$

where $a_{10} \in \mathcal{O}(-K_B)$, which is already of normal crossing type. From the multiplicity of vanishing of (f, g, Δ) at z = P = 0 there is an $A_{n-1} \to A_n$ enhancement, and we expect a single hypermultiplet in \mathbf{n} of $\mathrm{SU}(n)$. At $z = a_1 = 0$ there is an $A_{n-1} \to D_n$ enhancement, and we expect a single hypermultiplet in $\mathbf{\Lambda}^2$ of $\mathrm{SU}(n)$. These are well-known facts from perturbative string theory and can be deduced by either smoothing the singular geometry via small resolutions or deforming the 7-brane configuration [17, 33]. We will show how to obtain the correct spectrum without resolution or deformation. We note that our method for the computation of the matter works whether there exists a smooth or terminal Calabi-Yau minimal resolution, that is, our method is insensitive to the presence of terminal and not smooth singularities, as we can see from comparing with [32]. Therefore we will exclude the case I_1 as the singularity at the matter point is terminal and generically admits no

Fibration	Matter	Branes	M_L	$M_{\overline{L}}$	N
I_n fund		$\{\underline{\pi_1,\ldots,\pi_1},\pi_1\}$	$\begin{pmatrix} 1 & n+1 \\ 0 & 1 \end{pmatrix}$	$\begin{pmatrix} 1 & n-1 \\ 0 & 1 \end{pmatrix}$	1
	Λ^2	$\{\underline{\pi_1,\ldots,\pi_1},\pi_3,\pi_\beta,\pi_\alpha,\pi_2\}$	$\begin{pmatrix} 1 & n-8 \\ 0 & 1 \end{pmatrix}$	$\begin{pmatrix} 1 & n+8 \\ 0 & 1 \end{pmatrix}$	1
I_n^*	vect	$\{\underline{\pi_1, \pi_3, \pi_1, \pi_3, \pi_1, \pi_3, \pi_1, \cdots, \pi_1}, \pi_1, \pi_1\}$	$ \begin{pmatrix} -1 & n-2 \\ 0 & -1 \end{pmatrix} $		1
III	2	$\{\underline{\pi_1,\pi_3,\pi_2},\pi_1,\pi_3,\pi_2\}$	$\begin{pmatrix} -1 & 0 \\ 0 & -1 \end{pmatrix}$	$\mathrm{Id}_{2 imes2}$	2
IV_s	3	$\{\underline{\pi_1, \pi_3, \pi_1, \pi_3}, \pi_1, \pi_3, \pi_1, \pi_3\}$	$\begin{pmatrix} 0 & -1 \\ 1 & -1 \end{pmatrix}$	$\mathrm{Id}_{2 imes2}$	3
IV_s^*	27	$\{\underline{\pi_1, \pi_3, \pi_1, \pi_3, \pi_1, \pi_3, \pi_1, \pi_3}, \pi_1, \pi_3, \pi_1, \pi_3\}$	$\mathrm{Id}_{2 imes2}$	$\begin{pmatrix} -1 & 1 \\ -1 & 0 \end{pmatrix}$	1
III^*	56	$\{\underline{\pi_1, \pi_3, \pi_1, \pi_3, \pi_1, \pi_3, \pi_1, \pi_3, \pi_1, \pi_3, \pi_1, \pi_3, \pi_1, \pi_3}\}$	$\mathrm{Id}_{2 imes2}$	$ \begin{pmatrix} -1 & 0 \\ 0 & -1 \end{pmatrix} $	$\frac{1}{2}$
$III \times III$	(2, 2)	$\{\underline{\pi_1, \pi_3, \pi_2, \underline{\pi_1, \pi_3, \pi_2}}\}$	$\begin{pmatrix} -1 & 0 \\ 0 & -1 \end{pmatrix}$	$\mathrm{Id}_{2 imes2}$	1
$IV_s \times IV_s$	(3,3)	$\{\underline{\pi_1,\pi_3,\pi_1,\pi_3},\underline{\pi_1,\pi_3,\pi_1,\pi_3}\}$	$\begin{pmatrix} 0 & -1 \\ 1 & -1 \end{pmatrix}$	$\mathrm{Id}_{2 imes2}$	1
		$t: \{\underline{\pi_1, \pi_3, \pi_1, \pi_3}, \underline{\pi_1, \pi_3, \pi_1}, \pi_3\}$	$\begin{pmatrix} 0 & -1 \\ 1 & -1 \end{pmatrix}$	$\mathrm{Id}_{2 imes2}$	
$IV_s \times III$	R	$z: \{\underline{\pi_1, \pi_3, \pi_1}, \underline{\pi_1, \pi_3, \pi_1, \pi_3}, \pi_1, \pi_3\}$	$\begin{pmatrix} 0 & -1 \\ 1 & 0 \end{pmatrix}$	$\begin{pmatrix} 0 & 1 \\ -1 & 0 \end{pmatrix}$	1

Table 1. Summary of results. In each case we list the branes intersecting at the codimension 2 locus where the charged matters are localized and the monodromies corresponding to the branes. N is the multiplicity of the matter in the representation as listed in the second column of the table. The branes that carry the gauge algebra are underlined in the third column of the table. In the $IV_s \times III$ case $\mathbf{R} = (\mathbf{3}, \mathbf{2}) + (\mathbf{3}, \mathbf{1}) + (\mathbf{1}, \mathbf{2})$ and we will consider the brane contents and the monodromies on the t and z slices respectively and show that the results are consistent and match the anomaly cancellation condition in section 4.9.

crepant resolution though in this case one can obtain the correct (uncharged) localized matter spectrum at the matter point as expected from the perturbative limit. We will elaborate this point further in section 5. By constructing a type I_{ns} fiber using the Tate model, and then putting it into Weierstrass form, one can read off the roots of eq. (2.4) near z = 0, which take the form

$$x_1 = \frac{1}{12}a_{10}^2, \ x_2 = -\frac{1}{6}a_{10}^2, \ x_3 = \frac{1}{12}a_{10}^2.$$
 (4.2)

We see that x_1 and x_3 coincide therefore x_1 - x_3 can be fixed as the vanishing π_1 cycle along z=0. Along L_G we have $z=\epsilon e^{i\theta}$ and it is easy to show that on L_G we have $x_1-x_3\sim z^{\frac{n}{2}}$. This means that upon traversing z=0 once, the roots x_1 and x_3 have

Junction	SU(n) charge	a(J)
(1,0,0,0,0,-1)	(0,0,0,1)	(1,0)
(0,1,0,0,0,-1)	(0,0,1,-1)	(1,0)
(0,0,1,0,0,-1)	(0,1,-1,0)	(1,0)
(0,0,0,1,0,-1)	(1, -1, 0, 0)	(1,0))
(0,0,0,0,1,-1)	(-1,0,0,0)	(1,0)

Table 2. The 5 junctions corresponding to **5** of SU(5) near the point of enhancement z = P = 0. The middle column is the charge of the state under the Cartan U(1)'s of SU(5). a(J) is computed with respect to S_G . The 5 junctions corresponding to $\overline{\bf 5}$ are the orientation reversed junctions of the ones listed here.

swapped n times and that corresponds exactly to the monodromy $M_{L_G} = \begin{pmatrix} 1 & n \\ 0 & 1 \end{pmatrix}$. We therefore have $S_G = \{\pi_1, \dots, \pi_1\}$ where there are n π_1 's. It now remains to determine S_R and the monodromy of L_R for the two types of enhancement.

4.1.1 Matter in n

In this case L_R is centered at P=0 and is parameterized by $\delta e^{i\phi}$. It is easy to show that along L_R , $x_1-x_3\sim \delta^{\frac{1}{2}}e^{\frac{i\phi}{2}}$. Therefore upon traversing L_R , x_1 and x_3 swapped once hence the monodromy is $M_{L_R}=\begin{pmatrix} 1 & 1 \\ 0 & 1 \end{pmatrix}$. Therefore in this case $S_R=\{\pi_1\}$. We have $S_G+S_R=\{\pi_1,\ldots,\pi_1,\pi_1\}$ where there are n+1 π_1 's at z=P=0 hence there is a branching rule at the point of enhancement:

$$SU(n+1) \to SU(n)$$
:
 $adj_{SU(n+1)} \to adj_{SU(n)} + \mathbf{n} + \overline{\mathbf{n}} + \mathbf{1}$ (4.3)

There are n junctions with a(J) = (1,0) that give rise to \mathbf{n} and n junctions with a(J) = (-1,0) that give rise to $\overline{\mathbf{n}}$. To illustrate our method we compute the junctions explicitly using an SU(5) model and the result is listed in table 2.

The relevant matter-point monodromy matrices are:

$$M_1 = \begin{pmatrix} 1 & n+1 \\ 0 & 1 \end{pmatrix}, \qquad M_2 = \begin{pmatrix} 1 & n-1 \\ 0 & 1 \end{pmatrix}.$$
 (4.4)

We see that the a(J) = (1,0) junctions and the a(J) = (-1,0) junctions are preserved by M_1 and M_2 therefore no reduction is induced by the monodromy. Hence we obtain a hypermultiplet in \mathbf{n} of $\mathrm{SU}(n)$ at z = P = 0 as required by 6D anomaly cancellation.

4.1.2 Matter in Λ^2

This case can be worked out easily using perturbative string techniques but is subtle using our method. But we will see that the string junction description nicely reproduces the spectrum required by 6D anomaly cancellation.

In this case L_R is centered at $a_{10}=0$. Note that there are six solutions to $z=\tilde{\Delta}=0$ with respect to a_{10} but only four of them vanish when z=0 hence these are the four points inside L_R . We assume that $L_R=L_{R_4}\circ L_{R_3}\circ L_{R_2}\circ L_{R_1}$ where L_{R_i} is the loop enclosing $a_{10,i}$ inside L_R . It is easy to see that the geometric monodromy around L_R is an overall 4π rotation of x_1, x_2, x_3 with x_1 - x_3 rotated by -4π , i.e., swapped four times in an opposite direction with respect to the overall 4π rotation of the three roots. At first sight it might seem hard to derive what monodromy matrix it corresponds to but we can either geometrically show what the vanishing cycles are of the four relevant a_{10} 's hence derive the monodromy, or algebraically compare it with the well known result from perturbative string theory. We will see in this example that these two approaches nicely match each other.

We can choose an arbitrary type I_{ns} Tate model, for example, I_{5s} with SU(5) gauge algebra. The discriminant locus is of the form:

$$\Delta = z^5 \tilde{\Delta} = z^5 (a_{10}^4 P + a_{10}^2 K_1 z + K_2 z^2 + \mathcal{O}(z^3))$$
(4.5)

and f and g are of the form:

$$f = a_{10}Q_f(z) + \mathcal{O}(z^2),$$

 $g = a_{10}Q_g(z) + \mathcal{O}(z^3)$

where Q_f is linear in z and Q_q is quadratic in z.

Solving $\Delta = 0$ with respect to z there are 5 + k solutions where k is the order of Δ in z. Besides the five roots at z=0 that correspond to the five gauge branes, two of the remaining roots $z = z_A$ and $z = z_B$ approach z = 0 in the limit $a_{10} = 0$. It is easy to see from the forms of f, g and Δ that the $a_{10} = 0$ limit is the limit where the fiber becomes type I_{1s}^* and the gauge algebra becomes SO(10). In this sense the SU(5) gauge theory along z=0 is a Higgsing of the SO(10) gauge theory by a deformation parameterized by a_{10} . To match the result in perturbative string theory we must have that the branes at z=0 have vanishing cycles (1,0) and the two branes along $z=z_A$ and $z=z_B$ together form an O7 plane in the $a_{10} = 0$ limit. In the spirit of section 2 the $SL(2, \mathbb{Z})$ monodromy associated with the O7 plane stays the same under deformation. When a_{10} is small, the SO(10) theory is Higgsed and the branes z_A and z_B are separated from z=0 therefore we are able to choose a loop L_{A+B} around both $z=z_A$ and $z=z_B$ and the monodromy corresponding to this loop is the monodromy that corresponds to that of an O7 plane. It is now easy to see that upon going along L_{A+B} , the geometric motion of x_1, x_2, x_3 is an overall 2π rotation together with a -2π rotation of x_1 - x_3 . We see that the geometric monodromy corresponding to L_R is twice the geometric monodromy corresponding to an O7 plane. We know that

$$M_{O7} = \begin{pmatrix} -1 & 4\\ 0 & -1 \end{pmatrix}. \tag{4.6}$$

Therefore, according to eq. (3.3) we have:

$$M_{L_R} = \begin{pmatrix} 1 & -8 \\ 0 & 1 \end{pmatrix}. (4.7)$$

We also need to deduce the vanishing cycles corresponding to each of the four a_{10} 's inside L_R to read off the brane content on the disk D. This can be determined easily by observing that the geometric motion of x_1, x_2, x_3 around the loops $L_{R_2} \circ L_{R_1}$ and $L_{R_4} \circ L_{R_3}$ are both that of the loop around an O7 plane. Therefore we have

$$M_{L_{R_2} \circ L_{R_1}} = M_{L_{R_4} \circ L_{R_3}} = \begin{pmatrix} -1 & 4\\ 0 & -1 \end{pmatrix}.$$
 (4.8)

Geometrically it is a bit tricky to read off the vanishing cycles corresponding to $a_{10,2}$ and $a_{10,3}$ but it is pretty clear that the vanishing cycles associated with $a_{10,1}$ and $a_{10,4}$ are π_2 and π_3 by approaching these two points respectively. Therefore, according to eq. (3.3) we must have

$$M_{L_{R_2}}M_{\pi_2} = M_{\pi_3}M_{L_{R_3}} = \begin{pmatrix} -1 & 4\\ 0 & -1 \end{pmatrix}. \tag{4.9}$$

Therefore it can be determined that

$$M_{L_{R_2}} = \begin{pmatrix} 2 & 1 \\ -1 & 0 \end{pmatrix}, \ M_{L_{R_3}} = \begin{pmatrix} -1 & 4 \\ -1 & 3 \end{pmatrix}.$$
 (4.10)

Hence we can read off the vanishing cycles, $v_{a_{10,2}} = (1, -1)$, $v_{a_{10,3}} = (2, 1)$, and we have

$$S_G + S_R = \{\pi_1, \pi_1, \dots, \pi_1, \pi_3, \pi_\beta, \pi_\alpha, \pi_2\}$$
(4.11)

We can also read off the vanishing cycles directly from the geometry instead of using eq. (3.3). This requires looking at the elliptic fiber E which is a double cover of the x-plane branched at x_1, x_2, x_3 and the point at infinity instead of only looking at the x-plane.

In order to read off the vanishing cycles corresponding to $M_{L_{R_2}}$ and $M_{L_{R_3}}$, we note that these correspond to the collapse of v_2 as pictured in figure 6 instead of v_1 . Letting π_1 denote the vanishing cycle encircling the branch cut, we observe that the cycle v_2 simply corresponds to the image of a picard lefschetz monodromy acting on v_1 under a clockwise rotation of π_1 by 2π . Thus, letting T_{π_1} denote the matrix corresponding to the picard lefschetz monodromy, we conclude that $v_2 = T_{\pi_1}^{-2}v_1$. Performing the calculation in the canonical basis, we have $T_{\pi_1}^{-2} = \begin{pmatrix} 1 & -2 \\ 0 & 1 \end{pmatrix}$. Acting on the cycle $v_1 = (-1, -1)$, we find that this maps to $v_2 = (1, -1)$. A completely analogous calculation maps the cycle (0, 1) to (2, 1) via a counter-clockwise rotation, and we conclude.

Using the branes $S_G + S_R$ we can search for junctions that give rise to matters in this system. We will use SU(5) as a concrete example and we list the junctions corresponding to the highest weight state of Λ^2 in table 3.

The monodromy matrices M_L and $M_{\bar{L}}$ are both of the form $\begin{pmatrix} 1 & k \\ 0 & 1 \end{pmatrix}$ therefore the junctions with $a(J) = (\pm 2, 0)$ are invariant under their action. Hence it seems that there are $4 \ \Lambda^2$'s and $4 \ \overline{\Lambda^2}$'s to which the junctions correspond are the orientation reversed junctions of the ones that give rise to Λ^2 .

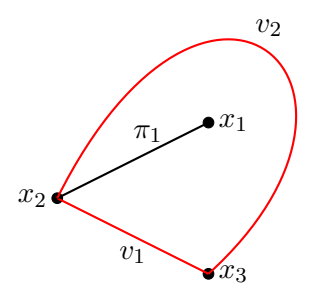


Figure 6. Ramification points away from infinity of the generic fiber. The black line denotes the choice of a branch cut, v_1 and v_2 correspond to two vanishing cycles with endpoints x_1 and x_2 .

Junction	SU(n) charge	a(J)
(1, 1, 0, 0, 0, -1, 1, -2, 2)	(0,0,1,0)	(2,0)
(1, 1, 0, 0, 0, 0, 0, -1, 1)	(0,0,1,0)	(2,0)
(1, 1, 0, 0, 0, 1, -1, 0, 0)	(0,0,1,0)	(2,0)
(1,1,0,0,0,2,-2,1,-1)	(0,0,1,0)	(2,0)

Table 3. The 4 junctions corresponding to the highest weight state of Λ^2 of SU(5) near the point of enhancement $z = a_{10} = 0$. The middle column is the charge of the state under the Cartan U(1)'s of SU(5). a(J) is computed with respect to S_G .

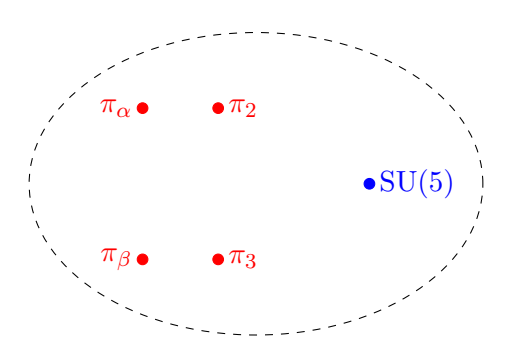


Figure 7. On disk D there are four I_1 's and the SU(5) gauge branes. The dashed curve denotes a closed (n,0) string that encloses the system $S_G + S_R$.

But in this case there is a subtlety that will also appear later when we discuss the type IV^* and type III^* models. We see that due to the form of the monodromy, there are closed eigen-strings that encloses the brane system $S_G + S_R$. Closed strings that carry charge (n,0) can enclose $S_G + S_R$ since (n,0) is invariant under the total monodromy M_L . This configuration is sketched in figure 7.

Here we see that the codimension 2 monodromy is:

$$M = \begin{pmatrix} 1 & k \\ 0 & 1 \end{pmatrix}. \tag{4.12}$$

The only charge vector a(J) with eigenvalue 1 under M is a(J) = (1,0) and indeed this is the only eigenvector of M. Since the eigenvalue is 1, a string emitting charge a(J) = (1,0)

can close back onto itself therefore becoming a closed string. We may call this an "closed eigen-string".

In particular we can choose a closed eigen-string that carries charge a(J) = (1,0). Via Hanany-Witten moves we can show that this closed eigen-string is equivalent to the junction

$$Q_C = \pm(0, 0, 0, 0, 0, 1, -1, 1, -1) \tag{4.13}$$

where the sign is determined by the direction of the charge running in the closed string. We choose J = (1, 1, 0, 0, 0, 1, -1, 0, 0) then we can see that all the other three junctions in table 3 are of the form $J + nQ_C$ where $n \in \mathbb{Z}$. Moreover, the intersection matrix corresponding to $S_G + S_R$ is:

$$I = \begin{pmatrix} -1 & 0 & 0 & 0 & \frac{1}{2} & \frac{1}{2} & -\frac{1}{2} & -\frac{1}{2} \\ 0 & -1 & 0 & 0 & 0 & \frac{1}{2} & \frac{1}{2} & -\frac{1}{2} & -\frac{1}{2} \\ 0 & 0 & -1 & 0 & 0 & \frac{1}{2} & \frac{1}{2} & -\frac{1}{2} & -\frac{1}{2} \\ 0 & 0 & 0 & -1 & 0 & \frac{1}{2} & \frac{1}{2} & -\frac{1}{2} & -\frac{1}{2} \\ 0 & 0 & 0 & 0 & -1 & \frac{1}{2} & \frac{1}{2} & -\frac{1}{2} & -\frac{1}{2} \\ \frac{1}{2} & \frac{1}{2} & \frac{1}{2} & \frac{1}{2} & \frac{1}{2} & -1 & -1 & -\frac{1}{2} & \frac{1}{2} \\ \frac{1}{2} & \frac{1}{2} & \frac{1}{2} & \frac{1}{2} & -1 & -1 & -\frac{3}{2} & -\frac{1}{2} \\ -\frac{1}{2} & -\frac{1}{2} & -\frac{1}{2} & -\frac{1}{2} & -\frac{1}{2} & -\frac{1}{2} & -\frac{3}{2} & -1 & -1 \\ -\frac{1}{2} & -\frac{1}{2} & -\frac{1}{2} & -\frac{1}{2} & -\frac{1}{2} & -\frac{1}{2} & -1 & -1 \end{pmatrix}.$$

$$(4.14)$$

To obtain a(J) = (2,0) junctions with respect to S_G , the following condition has to be satisfied:

$$n_1(0,1) + n_2(2,1) + n_3(1,-1) + n_4(-1,-1) = (-2,0)$$
 (4.15)

where $n_i \in \mathbb{N}$. We then have:

$$n_3 = \frac{1}{2}(n_1 - n_2) - 1, \ n_4 = \frac{1}{2}(n_1 + 3n_2) + 1.$$
 (4.16)

We then need to find $J=(J_G,n_1,n_2,n_3,n_4)$ such that (J,J)=-2 where J_G is a junction with $a(J_G)=(2,0)$ and $(J_G,J_G)=-2$ with respect to S_G . Solving (J,J)=-2 we have $n_2=-n_1$ or $n_2=1-n_1$. We see immediately that when $n_2=1-n_1$, n_3 and n_4 are not integers therefore we must have $n_2=-n_1$. Hence the junctions that give rise to Λ^2 are all of the form:

$$J = (J_G, n_1, -n_1, n_1 - 1, 1 - n_1) = (J_G, 1, -1, 0, 0) + (n_1 - 1)Q_C.$$

$$(4.17)$$

We have shown that Q_C is indeed a closed string so that all the junctions except those of the form $J = (J_G, 1, -1, 0, 0)$ are superpositions of a junction that stretches between S_G and S_R and a junction that is in fact a closed string. Therefore such states are not the matters that are localized at the point of enhancement and we are led to the conclusion that only one hypermultiplet in Λ^2 is the true localized matter at the point of enhancement. This matches the result that is required by 6D anomaly cancellation.

Junction	SO(8) charge	a(J)
(1,0,0,0,0,0,-1,0)	(0,0,0,1)	(1,0)
(1,0,0,0,0,0,0,-1)	(0,0,0,1)	(1,0)
(1, 1, -1, 0, -1, -1, 0, 1)	(0,0,0,1)	(-1,0)
(1, 1, -1, 0, -1, -1, 1, 0)	(0,0,0,1)	(-1,0)

Table 4. The four junctions with highest weight of $\mathbf{8}_{v}$ under SO(8).

4.2 Type I_n^*

In this case $S_G = \{\pi_1, \pi_3, \pi_1, \pi_3, \pi_1, \pi_3, \pi_1, \dots, \pi_1\}$ where there are in total n+6 branes. When n is even we have:

$$\Delta = z^{n+6} \left(a_{21}^2 \left(a_{4,2+\frac{n}{2}}^2 + P \right) + O(z) \right), \tag{4.18}$$

while when n is odd we have:

$$\Delta = z^{n+6} \left(a_{21}^3 a_{3,\frac{n+3}{2}}^2 + O(z) \right). \tag{4.19}$$

We consider first the locus where there is matter in **vect** as required by anomaly cancellation where $a_{4,2+\frac{n}{2}}=z=0$ (or $a_{3,\frac{n+3}{2}}=z=0$). The situation is exactly the same for the cases that n= even or the cases that n= odd therefore for simplicity we consider the case n=0. Here we require the gauge group to be SO(8) where we have:

$$\Delta = z^6 (a_{21}^2 (a_{21}^2 + P_1)(a_{21}^2 + P_2) + O(z)). \tag{4.20}$$

The matters are localized at $z = a_{21}^2 = 0$, $z = a_{21}^2 + P_1 = 0$ and $z = a_{21}^2 + P_2 = 0$. At $z = a_{21}^2 = 0$ the brane content is

 $S_G + S_R = \{\pi_1, \pi_3, \pi_1, \pi_3, \pi_1, \pi_3, \pi_1, \pi_1\}$ (4.21)

and we have:

$$M_L = \begin{pmatrix} -1 & -2 \\ 0 & -1 \end{pmatrix}, \qquad M_{\bar{L}} = \begin{pmatrix} -1 & 2 \\ 0 & -1 \end{pmatrix}.$$
 (4.22)

There are four sets of junctions in the representation $\mathbf{8}_{v}$ out of which the junctions with highest weights are given in table 4.

Upon the reductions given by eq. (4.22) we see that the matter content is $\mathbf{8}_{v} + \mathbf{8}_{v}$ which is the hypermultiplet in $\mathbf{8}_{v}$ of SO(8) as required by 6D anomaly cancellation.

The above lines of computations also apply to the other cases in the I_n^* series. For an I_n^* fiber at the locus $z=a_{4,2+\frac{n}{2}}=0$ the brane content is

$$S_G + S_R = \{\pi_1, \pi_3, \pi_1, \pi_3, \pi_1, \dots, \pi_1, \pi_1, \pi_1\}$$

$$(4.23)$$

where in $S_G + S_R$ there are in total n + 5 7-branes with π_1 vanishing cycle and the monodromies are:

$$M_L = \begin{pmatrix} -1 & n-2 \\ 0 & -1 \end{pmatrix}, \qquad M_{\bar{L}} = \begin{pmatrix} -1 & n+2 \\ 0 & -1 \end{pmatrix}.$$
 (4.24)

Junction	SO(8) charge	a(J)
(0,1,-1,-1,0,-1,-1,0)	(0,0,1,0)	(-1, -1)
(0,1,-1,-1,0,-1,0,-1)	(0,0,1,0)	(-1, -1)
(1, 1, 0, 0, 0, 0, 0, 1)	(0,0,1,0)	(1,1)
(1, 1, 0, 0, 0, 0, 1, 0)	(0,0,1,0)	(1, 1)

Table 5. The four junctions with highest weight of $\mathbf{8}_{s}$ under SO(8).

There are four sets of junctions in **vect** of SO(2n + 8) out of which there are two with a(J) = (1,0) and the other two with a(J) = (-1,0). Upon the reductions given by eq. (4.24) the matter content is a hypermultiplet in **vect** of SO(2n + 8) that meets the requirement of 6D anomaly cancellation.

The other locus $z = a_{21} = 0$ does not always exist for the type of elliptic fibration with I_n^* fibers considered here. Recall in fact that for I_n^* the Weierstrass model is:

$$\begin{split} f &= -3a_{21}^2z^2 + Fa_{21}z^3 + O(z^4), \\ g &= 2a_{21}^3z^3 + Ga_{21}^2z^4 + O(z^5), \\ \Delta &= z^{6+n}(a_{21}^2Q + O(z)). \end{split}$$

When $n \geq 4$ the order of vanishing of (f, g, Δ) at $z = a_{21} = 0$ exceeds (4, 6, 12) and this situation is beyond the scope of this paper.

When the locus $z = a_{21} = 0$ exists in I_n^* fibration, there will be matters in **spin** of SO(2n+8). We again use SO(8) as an example. In this example the matters are localized at $z = a_{21}^2 + P_1 = 0$ and $z = a_{21}^2 + P_2 = 0$. At $z = a_{21}^2 + P_1 = 0$ the brane content is:

$$S_G + S_R = \{\pi_1, \pi_3, \pi_1, \pi_3, \pi_1, \pi_3, \pi_2, \pi_2\}$$

$$(4.25)$$

and we have:

$$M_L = \begin{pmatrix} 1 & -2 \\ 2 & -3 \end{pmatrix}, \qquad M_{\bar{L}} = \begin{pmatrix} -3 & 2 \\ -2 & 1 \end{pmatrix}.$$
 (4.26)

There are four sets of junctions in the representation $\mathbf{8}_{s}$ out of which the junctions with highest weights are given in table 5.

At $z = a_{21}^2 + P_3 = 0$ the brane content is:

$$S_G + S_R = \{\pi_1, \pi_3, \pi_1, \pi_3, \pi_1, \pi_3, \pi_3, \pi_3\}$$

$$(4.27)$$

and we have:

$$M_L = \begin{pmatrix} -1 & 0 \\ 2 & -1 \end{pmatrix}, \qquad M_{\bar{L}} = \begin{pmatrix} -1 & 0 \\ -2 & -1 \end{pmatrix}.$$
 (4.28)

There are four sets of junctions in the representation $\mathbf{8}_{c}$ out of which the junctions with highest weights are given in table 6.

In both of the above two cases, it is easy to see that upon the reduction of the monodromies given by eq. (4.26) or eq. (4.28), the matter content is a hypermultiplet in either a hypermultiplet in $\mathbf{8}_{\rm c}$ which satisfies the requirement of 6D anomaly cancellation.

Junction	SO(8) charge	a(J)
(0,0,0,0,0,-1,0,1)	(1,0,0,0)	(0, -1)
(0,0,0,0,0,-1,1,0)	(1,0,0,0)	(0, -1)
(1, 1, 0, 1, -1, -1, -1, 0)	(1,0,0,0)	(0,1)
(11, 1, 0, 1, -1, -1, 0, -1)	(1,0,0,0)	(0,1)

Table 6. The four junctions with highest weight of $\mathbf{8}_{c}$ under SO(8).

4.3 Type *III*

The Weierstrass model we are using for type III is:

$$f = tz,$$

$$g = z^2 \tag{4.29}$$

of which the discriminant locus is:

$$\Delta = z^3 (27z + 4t^3). \tag{4.30}$$

The 7-branes near the point of enhancement z=t=0 are $S_G=\{\pi_1,\pi_3,\pi_2\}$ and $S_R=\{\pi_1,\pi_3,\pi_2\}$. Therefore there is a branching rule at the point of enhancement:

$$SO(8) \rightarrow SU(2)$$
:
 $\mathbf{28} \rightarrow \mathbf{3} + 4 \times (\mathbf{2} + \mathbf{2}) + 9 \times \mathbf{1}$ (4.31)

The junctions at the point of enhancement are listed in table 7.

The monodromy matrix M_L is that of type I_0^* , $M_L = \begin{pmatrix} -1 & 0 \\ 0 & -1 \end{pmatrix}$ while it is clear that $M_{\bar{L}}$ is trivial. The orbits of the asymptotic charges under M_L are:

Orbit 1:
$$(1,0) \to (-1,0)$$
 (4.32)

Orbit 2:
$$(1,1) \to (-1,-1)$$
 (4.33)

Both Orbit 1 and Orbit 2 give **2**. Out of the 8 **2**'s obtained from the branching rule, there are two of them with a(J) = (1,0), two of them with a(J) = (-1,0), two of them with a(J) = (-1,1) and two of them with a(J) = (-1,-1). The first two sets of junction are both on Orbit 1, and the latter two sets of junctions are both on Orbit 2. So after identifying the states via monodromy, there are 4 **2**'s left which become two **2** full hypers as required by 6D anomaly cancellation.

4.4 Type IV_s

The Weierstrass model we are using for type IV_s is:

$$f = z^2,$$

$$g = t^2 z^2$$

$$(4.34)$$

Junction	SU(2) charge	a(J)
(-1,-1,0,0,0,-1)	-1	(-1, -1)
(-1, -1, 0, 1, 1, 0)	-1	(-1,-1)
(-1,0,0,0,-1,-1)	-1	(-1,0)
(-1,0,0,1,0,0)	-1	(-1,0)
(0, -1, -1, -1, 0, 0)	-1	(1,0)
(0, -1, -1, 0, 1, 1)	-1	(1,0)
(0,0,-1,-1,-1,0)	-1	(1,1)
(0,0,-1,0,0,1)	-1	(1,1)
(0,0,1,0,0,-1)	1	(-1, -1)
(0,0,1,1,1,0)	1	(-1, -1)
(0,1,1,0,-1,-1)	1	(-1,0)
(0, 1, 1, 1, 0, 0)	1	(-1,0)
(1,0,0,-1,0,0)	1	(1,0)
(1,0,0,0,1,1)	1	(1,0)
(1, 1, 0, -1, -1, 0)	1	(1,1)
(1,1,0,0,0,1)	1	(1, 1)

Table 7. The 16 junctions near the point of enhancement $III \to I_0^*$. The middle column is the charge of the state under the Cartan U(1) of SU(2). a(J) is computed with respect to the first three 7-branes which are the gauge 7-branes.

of which the discriminant locus is:

$$\Delta = z^4 (4z^2 + 27t^4). \tag{4.35}$$

The 7-branes near the point of enhancement z=t=0 are $S_G=\{\pi_1,\pi_3,\pi_1,\pi_3\}$ and $S_R=\{\pi_1,\pi_3,\pi_1,\pi_3\}$. Therefore there is a branching rule at the point of enhancement:

$$E_6 \to SU(3)$$
: (4.36)

$$78 \to 8 + 9 \times (3 + \overline{3}) + 16 \times 1$$
 (4.37)

The monodromy matrix M_L is that of type IV^* , $M_L = \begin{pmatrix} 0 & -1 \\ 1 & -1 \end{pmatrix}$ while it is clear that $M_{\bar{L}}$ is trivial. The orbits of the asymptotic charges under M_L are:

Orbit 1:
$$(1,0) \to (0,1) \to (-1,-1) \to (1,0)$$
 (4.38)

Orbit 2:
$$(-1,0) \to (0,-1) \to (1,1) \to (-1,0)$$
 (4.39)

The junctions at the point of enhancement are listed in table 8.

Junction	SU(3) charge	a(J)
(-1, -1, 0, 0, 0, 0, 1, 1)	(-1,0)	(-1, -1)
(-1, -1, 0, 0, 1, 0, 0, 1)	(-1,0)	(-1, -1)
(-1, -1, 0, 0, 1, 1, 0, 0)	(-1,0)	(-1,-1)
(-1, -1, 1, 0, 0, 0, 0, 1)	(0,-1)	(0,-1)
(-1, -1, 1, 0, 0, 1, 0, 0)	(0,-1)	(0,-1)
(-1, -1, 1, 0, 1, 1, -1, 0)	(0,-1)	(0,-1)
(-1,0,0,-1,0,0,1,1)	(1,-1)	(-1, -1)
(-1,0,0,-1,1,0,0,1)	(1,-1)	(-1, -1)
(-1,0,0,-1,1,1,0,0)	(1,-1)	(-1, -1)
(-1,0,0,0,0,-1,1,1)	(0,-1)	(-1,0)
(-1,0,0,0,0,0,1,0)	(0, -1)	(-1,0)
(-1,0,0,0,1,0,0,0)	(0,-1)	(-1,0)
(0, -1, 0, 0, 0, 0, 0, 1)	(-1,1)	(0, -1)
(0, -1, 0, 0, 0, 1, 0, 0)	(-1,1)	(0, -1)
(0,-1,0,0,1,1,-1,0)	(-1,1)	(0, -1)
(0,-1,1,1,-1,0,0,0)	(-1,0)	(1,0)
(0, -1, 1, 1, 0, 0, -1, 0)	(-1,0)	(1,0)
(0, -1, 1, 1, 0, 1, -1, -1)	(-1,0)	(1,0)
(0,0,-1,-1,0,0,1,1)	(0,1)	(-1, -1)
(0,0,-1,-1,1,0,0,1)	(0, 1)	(-1, -1)
(0,0,-1,-1,1,1,0,0)	(0,1)	(-1, -1)
(0,0,-1,0,0,-1,1,1)	(-1,1)	(-1,0)
(0,0,-1,0,0,0,1,0)	(-1, 1)	(-1,0)
(0,0,-1,0,1,0,0,0)	(-1, 1)	(-1,0)
(0,0,0,-1,0,0,0,1)	(1,0)	(0, -1)
(0,0,0,-1,0,1,0,0)	(1,0)	(0, -1)
(0,0,0,-1,1,1,-1,0)	(1,0)	(0, -1)
(0,0,0,1,-1,-1,1,0)	(-1,0)	(0,1)
(0,0,0,1,0,-1,0,0)	(-1,0)	(0,1)
(0,0,0,1,0,0,0,-1)	(-1,0)	(0,1)
(0,0,1,0,-1,0,0,0)	(1, -1)	(1,0)
(0,0,1,0,0,0,-1,0)	(1, -1)	(1,0)
(0,0,1,0,0,1,-1,-1)	(1, -1)	(1,0)
(0,0,1,1,-1,-1,0,0)	(0, -1)	(1,1)
(0,0,1,1,-1,0,0,-1)	(0,-1)	(1,1)
(0,0,1,1,0,0,-1,-1)	(0, -1)	(1,1)
(0,1,-1,-1,0,-1,1,1)	(1,0)	(-1,0)
(0,1,-1,-1,0,0,1,0)	(1,0)	(-1,0)
(0,1,-1,-1,1,0,0,0)	(1,0)	(-1,0)
(0,1,0,0,-1,-1,1,0)	(1,-1)	(0,1)
(0,1,0,0,0,-1,0,0)	(1,-1)	(0,1)

(0, 1, 0, 0, 0, 0, 0, -1)	(1,-1)	(0,1)
(1,0,0,0,-1,0,0,0)	(0, 1)	(1,0)
(1,0,0,0,0,0,-1,0)	(0, 1)	(1,0)
(1,0,0,0,0,1,-1,-1)	(0, 1)	(1,0)
(1,0,0,1,-1,-1,0,0)	(-1, 1)	(1, 1)
(1,0,0,1,-1,0,0,-1)	(-1, 1)	(1, 1)
(1,0,0,1,0,0,-1,-1)	(-1, 1)	(1, 1)
(1, 1, -1, 0, -1, -1, 1, 0)	(0, 1)	(0,1)
(1, 1, -1, 0, 0, -1, 0, 0)	(0, 1)	(0,1)
(1, 1, -1, 0, 0, 0, 0, -1)	(0, 1)	(0, 1)
(1, 1, 0, 0, -1, -1, 0, 0)	(1,0)	(1, 1)
(1, 1, 0, 0, -1, 0, 0, -1)	(1,0)	(1, 1)
(1, 1, 0, 0, 0, 0, -1, -1)	(1,0)	(1, 1)

Table 8: The 54 junctions near the point of enhancement $IV_s \to IV^*$. The middle column is the charge of the state under the Cartan U(1)² of SU(3). a(J) is computed with respect to the first four 7-branes which are the gauge 7-branes.

Orbit 1 gives $\bf 3$ and Orbit 2 gives $\bf \overline{3}$. We first consider the 9 $\bf 3$'s. There are three of them with a(J)=(1,0), three of them with a(J)=(0,1) and three of them with a(J)=(-1,-1). We see that these three sets are all on Orbit 1 so after identifying states via monodromy, there are 3 $\bf 3$'s left. Next we consider the 9 $\bf \overline{3}$'s. There are three of them with a(J)=(1,1), three of them with a(J)=(0,-1) and three of them with a(J)=(-1,0). We see that these three sets are all on Orbit 2 so after identifying states via monodromy, there are 3 $\bf \overline{3}$'s left. In total there are 3 $\bf (3+\overline{3})$'s left which are the three full hypers required by 6D anomaly cancellation.

4.5 Type IV_s^*

The Weierstrass model we are using for type IV_s^* is:

$$f = z^3,$$

$$g = t^2 z^4$$

$$(4.40)$$

of which the discriminant locus is:

$$\Delta = z^8 (4z + 27t^4). \tag{4.41}$$

The 7-branes near the point of enhancement z = t = 0 are

$$S_G = \{\pi_1, \pi_3, \pi_1, \pi_3, \pi_1, \pi_3, \pi_1, \pi_3\}, S_R = \{\pi_1, \pi_3, \pi_1, \pi_3\}.$$

We see that there are 12 7-branes at codimension 2. The first eight 7-branes are the E_6 gauge branes and the last four 7-branes are the I_1 's associated with the solutions of $\tilde{\Delta} = 0$ with respect to g_4 . Near the enhancement point $z = g_4 = 0$ the geometry is sketched in figure 8.

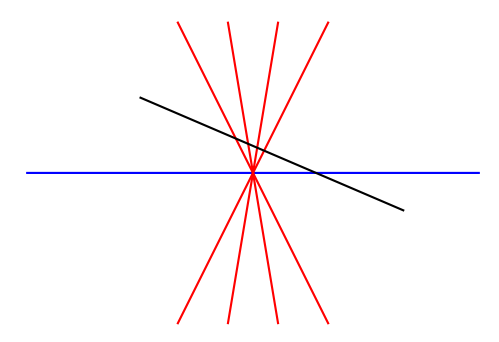
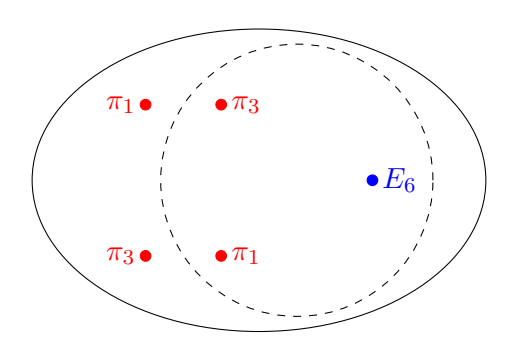


Figure 8. The gauge 7-branes of E_6 algebra are on top of each other and denoted by the red line. The four red lines denote the four I_1 's which are obtained from solving the equation $\tilde{\Delta} = 0$ with respect to g_4 . The black line segment denotes a disk D that intersects the 12 7-branes.



We choose a disk D that intersects the 12 7-branes near the enhancement point. On D the branes can be organized into a set of 10 7-branes that realizes an E_8 algebra and two extra branes π_1 and π_3 as shown in figure 9.

The branes in figure 8 can then be grouped to form the configuration shown in figure 10. We can see that because of their asymptotic charges, l_1 and l_3 can actually be deformed to junctions that loop around all the 12 7-branes via trivial Hanany-Witten moves since l_1 can be pulled across the branch cut of π_1 without creating a new prong and l_3 can be pulled across the branch cut of π_3 without creating a new prong. Via Hanany-Witten move we can show that l_1 is equivalent to the junction $Q_1 = (1, 1, 0, 1, -1, 0, -1, -1, 0, -1, 1, 0)$, l_3 is equivalent to the junction $Q_3 = (1, 0, 1, 1, 0, 1, -1, 0, -1, -1, 0, -1)$ and l_2 is equivalent to the junction $Q_2 = (2, 1, 1, 2, -1, 1, -2, -1, -1, -2, 1, -1)$. We can see that $Q_2 = Q_1 + Q_3$. Actually, all the junctions l_L that loop around all the 12 7-branes of this system is a superposition of l_1 and l_3 and its charge Q_L is a linear combination of Q_1 and Q_3 .

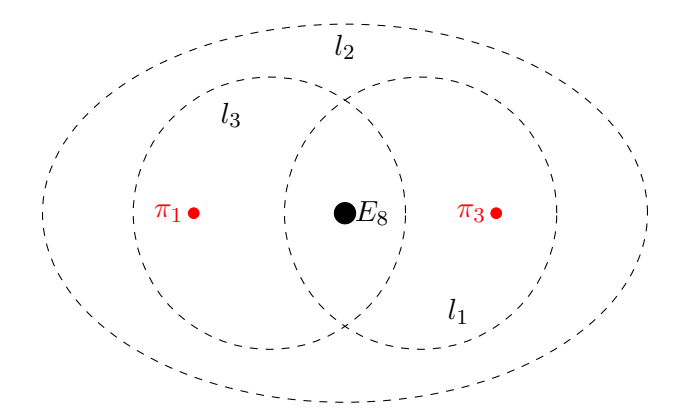


Figure 10. The E_8 branes obtained from the grouping together the E_6 gauge branes and the extra π_1 and π_3 branes are denoted by the big black point. l_1 is a junction that loops around the E_8 branes and a π_3 brane with charge $a(l_1) = (1,0)$. l_3 is a junction that loops around the E_8 branes and a π_1 brane with charge $a(l_3) = (0,1)$. l_2 is a junction that loops around all the 12 7-branes with charge $a(l_2) = (1,1)$.

The intersection matrix of this system with 12 7-branes is:

$$I = \begin{pmatrix} -1 & \frac{1}{2} & 0 & \frac{1}{2} \\ \frac{1}{2} & -1 & -\frac{1}{2} & 0 & -\frac{1}{2} & 0 & -\frac{1}{2} & 0 & -\frac{1}{2} & 0 & \frac{1}{2} & 0 \\ 0 & -\frac{1}{2} & -1 & \frac{1}{2} & 0 & \frac{1}{2} & 0 & \frac{1}{2} & 0 & \frac{1}{2} & 0 & \frac{1}{2} \\ \frac{1}{2} & 0 & \frac{1}{2} & -1 & -\frac{1}{2} & 0 & -\frac{1}{2} & 0 & -\frac{1}{2} & 0 & \frac{1}{2} \\ 0 & -\frac{1}{2} & 0 & -\frac{1}{2} & -1 & \frac{1}{2} & 0 & \frac{1}{2} & 0 & \frac{1}{2} & 0 & \frac{1}{2} \\ \frac{1}{2} & 0 & \frac{1}{2} & 0 & \frac{1}{2} & -1 & -\frac{1}{2} & 0 & -\frac{1}{2} & 0 & \frac{1}{2} \\ 0 & -\frac{1}{2} & 0 & -\frac{1}{2} & 0 & -\frac{1}{2} & -1 & \frac{1}{2} & 0 & \frac{1}{2} & 0 & \frac{1}{2} \\ \frac{1}{2} & 0 & \frac{1}{2} & 0 & \frac{1}{2} & 0 & \frac{1}{2} & -1 & -\frac{1}{2} & 0 & \frac{1}{2} \\ 0 & -\frac{1}{2} & 0 & -\frac{1}{2} & 0 & -\frac{1}{2} & 0 & -\frac{1}{2} & -1 & -\frac{1}{2} & 0 \\ 0 & -\frac{1}{2} & 0 & -\frac{1}{2} & 0 & -\frac{1}{2} & 0 & -\frac{1}{2} & -1 & -\frac{1}{2} & 0 \\ 0 & -\frac{1}{2} & 0 & -\frac{1}{2} & 0 & -\frac{1}{2} & 0 & -\frac{1}{2} & -1 & -\frac{1}{2} & 0 \\ 0 & -\frac{1}{2} & 0 & -\frac{1}{2} & 0 & -\frac{1}{2} & 0 & -\frac{1}{2} & -1 & -\frac{1}{2} & 0 \\ 0 & -\frac{1}{2} & 0 & -\frac{1}{2} & 0 & -\frac{1}{2} & 0 & -\frac{1}{2} & -1 & -\frac{1}{2} & 0 \\ 0 & -\frac{1}{2} & 0 & -\frac{1}{2} & 0 & -\frac{1}{2} & 0 & -\frac{1}{2} & -1 & -\frac{1}{2} & 0 \\ 0 & -\frac{1}{2} & 0 & -\frac{1}{2} & 0 & -\frac{1}{2} & 0 & -\frac{1}{2} & -1 & -\frac{1}{2} & 0 \\ 0 & -\frac{1}{2} & 0 & -\frac{1}{2} & 0 & -\frac{1}{2} & 0 & -\frac{1}{2} & -1 & -\frac{1}{2} & 0 \\ 0 & -\frac{1}{2} & 0 & -\frac{1}{2} & 0 & -\frac{1}{2} & 0 & -\frac{1}{2} & -1 & -\frac{1}{2} & 0 \\ 0 & -\frac{1}{2} & 0 & -\frac{1}{2} & 0 & -\frac{1}{2} & 0 & -\frac{1}{2} & -1 & -\frac{1}{2} & 0 \\ 0 & -\frac{1}{2} & -1 & -\frac{1}{2} & 0 \\ 0 & -\frac{1}{2} & -1 & -\frac{1}{2} & 0 \\ 0 & -\frac{1}{2} & -1 & -\frac{1}{2} & 0 \\ 0 & -\frac{1}{2} & -1 & -\frac{1}{2} & 0 \\ 0 & -\frac{1}{2} & -1 & -\frac{1}{2} & 0 \\ 0 & -\frac{1}{2} & -1 &$$

It is easy to show that with respect to I the self-intersection numbers $(l_1, l_1) = (l_2, l_2) = (l_3, l_3) = 0$. The junctions correspond to the simple roots of E_8 are:

$$\begin{split} &\alpha_1 = (0,0,0,1,-1,-1,0,-1,1,1,0,0),\\ &\alpha_2 = (0,0,0,0,0,0,0,1,0,-1,0,0),\\ &\alpha_3 = (0,0,0,0,0,0,1,0,-1,0,0,0),\\ &\alpha_4 = (0,0,0,0,1,0,-1,0,0,0,0,0),\\ &\alpha_5 = (0,0,1,0,-1,0,0,0,0,0,0,0),\\ &\alpha_6 = (0,1,-2,-1,0,-1,1,0,1,1,0,0),\\ &\alpha_7 = (1,-1,1,1,0,1,-1,0,-1,-1,0,0),\\ &\alpha_8 = (0,0,0,0,0,1,-1,-1,1,0,0,0). \end{split}$$

It is easy to show that $(a_i, l_1) = (a_i, l_2) = (a_i, l_3) = 0$. Since any root γ of E_8 can be written as $\gamma = \sum_i a_i \alpha_1$ with $(\gamma, \gamma) = -2$ and any junction l_L that loop around all the 12

7-branes can be written as $l_L = Al_1 + Bl_3$, we see that $(l_L, l_L) = 0$, $(\gamma, l_L) = 0$ therefore $(\gamma + nl_L, \gamma + nl_L) = -2$, where a_i , A, B and n are all integers. We denote by J_n the states $\gamma + nl_L$. It is obvious that $a(J_n) = (0,0)$.

Moreover, $S_g = \{\alpha_1, \alpha_2, \alpha_3, \alpha_4, \alpha_5, \alpha_6, \alpha_7, \alpha_8, l_1, l_3\}$ is a set that generates all the junctions with a(J) = (0,0). So that all the junctions with a(J) = (0,0) and (J,J) = -2 are of the form $\gamma + nl_L$ since $a(l_L) = 0$ and $(l_L, \psi) = 0$, $\forall \psi \in S_g$ and the only linear combinations of α_i 's such that $(\sum_i c_i \alpha_i, \sum_i c_i \alpha_i) = -2$ and $a(\sum_i a_i \alpha_i) = (0,0)$ are the roots of E_8 , γ .

Now we see that there is an infinite number of states $J_n = \gamma + nl_L$ such that $a(J_n) = (0,0)$ and $(J_n,J_n) = -2$ that are graded by n. For $n \neq 0$, J_n is a junction that is a superposition of a junction γ that stretches between E_6 gauge branes and the I_1 locus and a junction l_L that is a closed string around the 12 7-branes of the system. These states are not the matters that are localized at the enhancement point at codimension 2 on the base. To extract only the matter content at codimension 2, we need to focus on the junctions J_0 , i.e., γ 's that stretch between the E_6 gauge branes and the I_1 locus without being superposed with a closed string l_L .

Therefore in this system what we actually have is an enhancement from E_6 to E_8 , the string junctions can be derived via the branching rule:

$$E_8 \to E_6$$
: (4.43)

$$248 \rightarrow 78 + 3 \times (27 + \overline{27}) + 8 \times 1$$
 (4.44)

The relevant monodromies are:

$$M_{L_R} = \begin{pmatrix} -1 & 1 \\ -1 & 0 \end{pmatrix}, \ M_{L_G} = \begin{pmatrix} 0 & -1 \\ 1 & -1 \end{pmatrix}.$$
 (4.45)

Therefore we have:

$$M_L = \begin{pmatrix} 1 & 0 \\ 0 & 1 \end{pmatrix}, \ M_{\bar{L}} = \begin{pmatrix} -1 & 1 \\ -1 & 0 \end{pmatrix}$$
 (4.46)

We see that M_L is trivial and the orbit of $M_{\bar{L}}$ is:

Orbit:
$$(1,0) \to (-1,-1) \to (0,1) \to (1,1) \to (0,-1)$$
 (4.47)

Out of the three full hypers in 27, one of them is with $a(J) = (\pm 1, 0)$, one the them with $a(J) = \pm (1, 1)$ and one of them with $a(J) = (0, \pm 1)$. We see that all of them are on the orbit of either $M_{\bar{L}}$ so they will be identified via the monodromy and there is only one full hyper in 27 left in the spectrum which is the matter content required by 6D anomaly cancellation.

4.6 Type *III**

The Weierstrass model we are using for type III^* is:

$$f = tz^3,$$

$$g = z^5$$

$$(4.48)$$

of which the discriminant locus is:

$$\Delta = z^9 (27z + 4t^3). \tag{4.49}$$

The 7-branes near the point of enhancement z = t = 0 are:

$$S_G = \{\pi_1, \pi_3, \pi_1, \pi_3, \pi_1, \pi_3, \pi_1, \pi_3, \pi_1\}, S_R = \{\pi_3, \pi_1, \pi_3\}.$$

By comparing with the result in section 4.5 we see that near the z = t = 0 the brane content $S_G + S_R$ is exactly the same as that of type IV^* . It is clear that the argument in section 4.5 also holds in this case since it only uses the data of the brane content on the disk D but not the details of the Weierstrass model. Therefore in this case the gauge algebra is also effectively enhanced to E_8 . Hence we have the branching rule:

$$E_8 \to E_7$$

248 \to **133** + 2 × **56** + 3. (4.50)

The relevant monodromies are:

$$M_{L_R} = \begin{pmatrix} 0 & 1 \\ -1 & 0 \end{pmatrix}, \ M_{L_G} = \begin{pmatrix} 0 & 1 \\ -1 & 0 \end{pmatrix}.$$
 (4.51)

Therefore we have:

$$M_L = \begin{pmatrix} 1 & 0 \\ 0 & 1 \end{pmatrix}, \ M_{\bar{L}} = \begin{pmatrix} -1 & 0 \\ 0 & -1 \end{pmatrix} \tag{4.52}$$

We see that M_L is trivial and the orbit of $M_{\bar{L}}$ is:

Orbit:
$$(0,1) \to (0,-1) \to (0,1)$$
. (4.53)

The two **56**'s obtained from string junction computation are one with a(J) = (0,1) and one with a(J) = (-1,0). We see that they are on the orbit of $M_{\bar{L}}$ so they are identified. We are left with one **56** that forms half hypermultiplet in **56** of E_7 . This is the matter content that is required by 6D anomaly cancellation.

4.7 *III* × *III*

The Weierstrass model we are using for type $III \times III$ is:

$$f = zt,$$

$$g = z^2 t^2$$

$$(4.54)$$

of which the discriminant locus is:

$$\Delta = z^3 t^3 (4 + 27zt). \tag{4.55}$$

The 7-branes near the intersection point z = t = 0 are:

$$S_G = \{\pi_1, \pi_3, \pi_2, \pi_1, \pi_3, \pi_2\}.$$

It is easy to see the branching rule is:

$$SO(8) \to SU(2) \times SU(2) :$$

 $\mathbf{28} \to (\mathbf{3}, \mathbf{1}) + (\mathbf{1}, \mathbf{3}) + 4 \times (\mathbf{2}, \mathbf{2}) + 6 \times (\mathbf{1}, \mathbf{1}).$

Note that there are two sets of gauge 7-branes S_A and S_B , therefore we label the asymptotic charge of the junctions by $a(J) = (Q_A, Q_B)$ where Q_A is the asymptotic charge associated with S_A and Q_B the asymptotic charge associated with S_B .

The $4(\mathbf{2}, \mathbf{2})$ are respectively with asymptotic charge:

$$a(J_1) = ((1,0), (-1,0)),$$

$$a(J_2) = ((-1,0), (1,0)),$$

$$a(J_3) = ((1,1), (-1,-1)),$$

$$a(J_4) = ((-1,-1), (1,1)).$$

We have:

$$M_L = \begin{pmatrix} -1 & 0 \\ 0 & -1 \end{pmatrix}, \quad M_{\bar{L}} = \begin{pmatrix} 1 & 0 \\ 0 & 1 \end{pmatrix}. \tag{4.56}$$

Therefore we have $J_1 \to J_2$ and $J_3 \to J_4$ under the monodromies M_L and $M_{\bar{L}}$. This gives rise to one hypermultiplet in the bifundamental representation of $SU(2) \times SU(2)$ which matches the result of 6D anomaly cancellation.

4.8 $IV_s \times IV_s$

The Weierstrass model we are using for type $IV_s \times IV_s$ is:

$$f = z^2 t^2,$$

$$q = z^2 t^2$$

$$(4.57)$$

of which the discriminant locus is:

$$\Delta = z^4 t^4 (27 + 4z^2 t^2). \tag{4.58}$$

The 7-branes near the intersection point z = t = 0 are:

$$S_G = \{\pi_1, \pi_3, \pi_1, \pi_3, \pi_1, \pi_3, \pi_1, \pi_3\}.$$

It is easy to see the branching rule is:

$$E_6 \to SU(3) \times SU(3) :$$

 $\mathbf{78} \to (\mathbf{8}, \mathbf{1}) + (\mathbf{1}, \mathbf{8}) + 3 \times ((\mathbf{3}, \overline{\mathbf{3}}) + (\overline{\mathbf{3}}, \mathbf{3})) + 8 \times (\mathbf{1}, \mathbf{1}).$

Again there are two sets of gauge 7-branes S_A and S_B , therefore we label the asymptotic charge of the junctions by $a(J) = (Q_A, Q_B)$ where Q_A is the asymptotic charge associated with S_A and Q_B the asymptotic charge associated with S_B .

The 3 $(3, \overline{3})$ are respectively with asymptotic charge:

$$a(J_1) = ((1,0), (-1,0)),$$

 $a(J_2) = ((0,1), (0,-1)),$
 $a(J_3) = ((-1,-1), (1,1)).$

And the $3(\overline{\bf 3}, {\bf 3})$ are respectively with asymptotic charge:

$$a(J_4) = ((-1,0), (1,0)),$$

 $a(J_5) = ((0,-1), (0,1)),$
 $a(J_6) = ((1,1), (-1,-1)).$

We have:

$$M_L = \begin{pmatrix} 0 & -1 \\ 1 & -1 \end{pmatrix}, \quad M_{\bar{L}} = \begin{pmatrix} 1 & 0 \\ 0 & 1 \end{pmatrix}. \tag{4.59}$$

Therefore we have $J_1 \to J_2 \to J_3$ and $J_4 \to J_5 \to J_6$ under the monodromies M_L and $M_{\bar{L}}$. This gives rise to one hypermultiplet in the bifundamental representation of $SU(3) \times SU(3)$ which matches the result of 6D anomaly cancellation.

4.9 $IV_s \times III$

The Weierstrass model we are using for type $IV_s \times III$ is:

$$f = zt^2,$$

$$g = z^2t^2$$

$$(4.60)$$

of which the discriminant locus is:

$$\Delta = z^3 t^4 (4t^2 + 27z) \tag{4.61}$$

We will consider two natural 7-brane systems corresponding to the triple intersection dictated by the discriminant locus. Consider the brane system corresponding to the t-slice:

$$S_{G_t} = \{\pi_1, \pi_3, \pi_1, \pi_3, \pi_1, \pi_3, \pi_1, \pi_3\}.$$

The corresponding branching rule at the point of enhancement is:

$$E_6 \to SU(3) \times SU(2) :$$
 $\mathbf{78} \to (\mathbf{8}, \mathbf{1}) + (\mathbf{1}, \mathbf{3}) + 3 \times ((\mathbf{3}, \mathbf{2}) + (\overline{\mathbf{3}}, \mathbf{2})) + 3 \times ((\mathbf{3}, \mathbf{1}) + (\overline{\mathbf{3}}, \mathbf{1})) + ((\mathbf{1}, \mathbf{2}) + (\mathbf{1}, \mathbf{2})) + 9 \times (\mathbf{1}, \mathbf{1})$

The monodromy matrix of this system is identical to that of type $IV_s \times IV_s$,

$$M_L = \begin{pmatrix} 0 & -1 \\ 1 & -1 \end{pmatrix}, \quad M_{\bar{L}} = \begin{pmatrix} 1 & 0 \\ 0 & 1 \end{pmatrix}. \tag{4.62}$$

As in the above, there are two sets of gauge 7-branes S_A and S_B , but a novelty of the $IV_s \times III$ model is that there is an extra I_1 brane (or two extra I_1 branes as we will see momentarily) therefore we will label the corresponding asymptotic charges of the junctions by $a(J) = (Q_A, Q_B, Q_{I_1})$ with Q_A the asymptotic charge with respect to S_A , Q_B the asymptotic charge with respect to S_B and Q_{I_1} with respect to the extra I_1 .

This induces a partition of the set $S_{G_t} = \{S_A, S_B, I_1\}$, where S_A is the first 4 branes in S_{G_t} corresponding to the locus $t^4 = 0$ and the set $\{S_B, I_1\}$ denote the intersection of the SU(2) and I_1 seven-brane intersections with the t-slice.

We will consider only the subset of junctions charged under S_A and the action of the monodromy M with respect to the asymptotic charge Q_A . The 3 (3,1) carry the asymptotic charges:

$$a(J_1) = ((0,1)_A, (0,0)_B, (0,-1)_{I_1}),$$

$$a(J_2) = ((-1,-1)_A, (1,1)_B, (0,0)_{I_1}),$$

$$a(J_3) = ((1,0)_A, (-1,1)_B, (0,-1)_{I_1}).$$

while the 3(3,2) carry the asymptotic charges:

$$a(J_4) = ((0,1)_A, (0,-1)_B, (0,0)_{I_1}),$$

$$a(J_5) = ((-1,-1)_A, (1,0)_B, (0,1)_{I_1}),$$

$$a(J_6) = ((1,0)_A, (-1,0)_B, (0,0)_{I_1}).$$

Therefore we have $J_1 \to J_2 \to J_3$ and $J_4 \to J_5 \to J_6$ under the monodromies M_L and $M_{\bar{L}}$. This gives rise to one hypermultiplet in the (3,1) and one hypermultiplet in the bifundamental representation of SU(3) × SU(2) which matches the result of 6D anomaly cancellation.

Instead, taking the brane system corresponding to the z-slice, we have the following:

$$S_{G_z} = \{\pi_1, \pi_3, \pi_1, \pi_1, \pi_3, \pi_1, \pi_3, \pi_1, \pi_3\}.$$

The corresponding branching rule at the point of enhancement is:

$$E_7 \to SU(3) \times SU(2) :$$

 $\mathbf{133} \to (\mathbf{8}, \mathbf{1}) + (\mathbf{1}, \mathbf{3}) + 4 \times ((\mathbf{3}, \mathbf{2}) + (\overline{\mathbf{3}}, \mathbf{2})) + 7 \times ((\mathbf{3}, \mathbf{1}) + (\overline{\mathbf{3}}, \mathbf{1}))$
 $+ 4 \times ((\mathbf{1}, \mathbf{2}) + (\mathbf{1}, \mathbf{2})) + 16 \times (\mathbf{1}, \mathbf{1})$

The monodromy matrix of this system is given by

$$M_L = \begin{pmatrix} 0 & -1 \\ 1 & 0 \end{pmatrix}, \quad M_{\bar{L}} = \begin{pmatrix} 0 & 1 \\ -1 & 0 \end{pmatrix}. \tag{4.63}$$

With notation as in the above, this set of 7-branes is naturally partitioned as $S_{G_z} = \{S_B, S_A, I_1\}$ where we now have the set $\{S_A, I_1\}$ denoting the intersection of the SU(3) and

2 I_1 seven-brane intersections with the z-slice. The 8 (1,2) carry the asymptotic charges:

$$a(J_1) = ((0,0)_B, (0,-1)_A, (0,1)_{I_1}),$$

$$a(J_2) = ((1,2)_B, (0,-1)_A, (-1,-1)_{I_1}),$$

$$a(J_3) = ((0,0)_B, (-1,0)_A, (1,0)_{I_1}),$$

$$a(J_4) = ((1,-1)_B, (-1,0)_A, (0,1)_{I_1}),$$

$$a(J_5) = ((0,0)_B, (0,1)_A, (0,-1)_{I_1}),$$

$$a(J_6) = ((-1,-2)_B, (0,1)_A, (1,1)_{I_1}),$$

$$a(J_7) = ((0,0)_B, (1,0)_A, (-1,0)_{I_1}),$$

$$a(J_8) = ((-1,1)_B, (1,0)_A, (0,-1)_{I_1}),$$

while the 4 (3,2) carry the asymptotic charges:

$$a(J_9) = ((0,1)_B, (0,-1)_A, (0,0)_{I_1}),$$

$$a(J_{10}) = ((1,0)_B, (-1,0)_A, (0,0)_{I_1}),$$

$$a(J_{11}) = ((0,1)_B, (1,0)_A, (-1,-1)_{I_1}),$$

$$a(J_{12}) = ((-1,-1)_B, (0,1)_A, (1,0)_{I_1}),$$

Therefore we have $\{J_1, J_2\} \to \{J_3, J_4\} \to \{J_5, J_6\} \to \{J_7, J_8\}$ and $J_9 \to J_{10} \to J_{11} \to J_{12}$ under the monodromies M_L and $M_{\bar{L}}$. This gives rise to one hypermultiplet in the $(\mathbf{1}, \mathbf{2})$ and one hypermultiplet in the bifundamental representation of $\mathrm{SU}(3) \times \mathrm{SU}(2)$.

Combining the results from the different slices, we find in total a charged hypermultiplet spectrum of $(\mathbf{3}, \mathbf{2}) + (\mathbf{3}, \mathbf{1}) + (\mathbf{1}, \mathbf{2})$, matching the anomaly cancelling spectrum of [19]. Note that the bifundamental massless spectrum computed from the z-slice is the same state computed from the t-slice and hence is consistent with expectations.

5 Remarks on localized neutral hypermultiplets

In section 4.1 we noted that our method for the computation of the matter works whether there exists a smooth or terminal Calabi-Yau minimal resolution, that is, our method is insensitive to the presence of terminal and not smooth singularities, as we can see from comparing with [26, 32]. However, we remark that our method, in general, does not necessarily yield the correct uncharged matter spectrum away from the perturbative limit.

Our theory computes the localized charged matter spectrum at the intersection of seven-branes. However, localized neutral hypermultiplets may also exist [26]. We would like to comment on localized neutral hypermultiplets in light of our prescription. In particular, we will argue that more information must be added to our prescription to account for the appearance of localized neutral hypermultiplets.

In [26], the physical significance of non-crepant resolvable singularities on an elliptically fibered Calabi-Yau threefold X was investigated from the perspective of a 6d F-theory compactification. The central result asserts that after passing to a \mathbb{Q} -factorial terminal

model $\hat{X} \to X$, the total number of localized, massless neutral hypermultiplets on the resulting M-theory Coulomb branch is given by the sum

$$n_H^0 = \sum_P m_P$$

over singular points of \hat{X} where m_P is the Milnor number. Moreover, this proposal was demonstrated to be consistent with 6d gravitational anomaly cancellation and naturally appears as a summand of the total space of complex structure deformations of \hat{X} .

To demonstrate that our prescription is insensitive to the presence of localized neutral hypermultiplets, we will focus on the examples explored in ([26], section 5.1). Consider a type III-model with the following tunings:

$$f = z_1 f_0$$
, $g = z_1^{\mu_g} g_0$ for $\mu_g \ge 2$, $\Delta = z_1^3 (4f_0^3 + 27z_1^{2\mu_g - 3}g_0^2)$

As demonstrated in loc cit., for $\mu_g = 2, 3$, the model admits a crepant resolution, while for $\mu_g \geq 4$, the partial resolution exhibits a terminal hypersurface singularity. In particular, for $\mu_g = 4, 5, 7$, the isolated singularity results in the milnor numbers $\mu = 1, 2, 4$ respectively.

On the other hand, our prescription applied to the type III model in section 4.3, is insensitive to higher order terms in z_1 in the residual discriminant. In particular, our proposed brane content, monodromies, and calculation of junction states would yield precisely the same matter content in any of the above tuned models as in the generic case with $\mu_g = 2$.

Therefore, we conclude that our prescription is incomplete in accounting for localized neutral matter, and we leave this avenue of investigation for future work.

Acknowledgments

We thank Bobby Acharya, Sakura Schafer-Nameki, Yi-Nan Wang and Timo Weigand for discussions. J.H. is supported by NSF CAREER grant PHY-1848089. The work of C.L. was partially supported by the Alfred P. Sloan Foundation Grant No. G-2019-12504 and by DOE Grant DE-SC0013607. B.S. is supported by the NSF Graduate Research Fellowship under grant DGE-1451070. J.T. is supported by a grant from the Simons Foundation (#488569, Bobby Acharya). This material is in part based upon work supported by the NSF Grant DMS-1440140 while A.G. was in residence at the Mathematical Sciences Research Institute in Berkeley, California, during the Spring 2019 semester; AG gratefully acknowledges the support of a Simons Fellowship. The work of A.G. is partially supported by PRIN "Moduli and Lie Theory". A.G. is a member of GNSAGA of INDAM.

Open Access. This article is distributed under the terms of the Creative Commons Attribution License (CC-BY 4.0), which permits any use, distribution and reproduction in any medium, provided the original author(s) and source are credited. SCOAP³ supports the goals of the International Year of Basic Sciences for Sustainable Development.

References

- [1] C. Vafa, Evidence for F-theory, Nucl. Phys. B 469 (1996) 403 [hep-th/9602022] [INSPIRE].
- [2] D.R. Morrison and C. Vafa, Compactifications of F-theory on Calabi-Yau threefolds. 2, Nucl. Phys. B 476 (1996) 437 [hep-th/9603161] [INSPIRE].
- [3] M. Bershadsky, K.A. Intriligator, S. Kachru, D.R. Morrison, V. Sadov and C. Vafa, Geometric singularities and enhanced gauge symmetries, Nucl. Phys. B 481 (1996) 215 [hep-th/9605200] [INSPIRE].
- [4] S.H. Katz and C. Vafa, Geometric engineering of N=1 quantum field theories, Nucl. Phys. B 497 (1997) 196 [hep-th/9611090] [INSPIRE].
- [5] D.R. Morrison and W. Taylor, Matter and singularities, JHEP 01 (2012) 022[arXiv:1106.3563] [INSPIRE].
- [6] S. Katz, D.R. Morrison, S. Schäfer-Nameki and J. Sully, Tate's algorithm and F-theory, JHEP 08 (2011) 094 [arXiv:1106.3854] [INSPIRE].
- [7] M. Esole and S.-T. Yau, Small resolutions of SU(5)-models in F-theory, Adv. Theor. Math. Phys. 17 (2013) 1195 [arXiv:1107.0733] [INSPIRE].
- [8] J. Marsano and S. Schäfer-Nameki, Yukawas, G-flux, and Spectral Covers from Resolved Calabi-Yau's, JHEP 11 (2011) 098 [arXiv:1108.1794] [INSPIRE].
- [9] C. Lawrie and S. Schäfer-Nameki, *The Tate Form on Steroids: Resolution and Higher Codimension Fibers*, *JHEP* **04** (2013) 061 [arXiv:1212.2949] [INSPIRE].
- [10] H. Hayashi, C. Lawrie, D.R. Morrison and S. Schäfer-Nameki, Box Graphs and Singular Fibers, JHEP 05 (2014) 048 [arXiv:1402.2653] [INSPIRE].
- [11] D. Klevers, D.K. Mayorga Pena, P.-K. Oehlmann, H. Piragua and J. Reuter, F-Theory on all Toric Hypersurface Fibrations and its Higgs Branches, JHEP **01** (2015) 142 [arXiv:1408.4808] [INSPIRE].
- [12] M.R. Gaberdiel and B. Zwiebach, Exceptional groups from open strings, Nucl. Phys. B 518 (1998) 151 [hep-th/9709013] [INSPIRE].
- [13] O. DeWolfe, T. Hauer, A. Iqbal and B. Zwiebach, Constraints on the BPS spectrum of N=2, D=4 theories with A-D-E flavor symmetry, Nucl. Phys. B **534** (1998) 261 [hep-th/9805220] [INSPIRE].
- [14] O. DeWolfe and B. Zwiebach, String junctions for arbitrary Lie algebra representations, Nucl. Phys. B **541** (1999) 509 [hep-th/9804210] [INSPIRE].
- [15] M. Cvetič, I. Garcia-Etxebarria and J. Halverson, Global F-theory Models: Instantons and Gauge Dynamics, JHEP 01 (2011) 073 [arXiv:1003.5337] [INSPIRE].
- [16] M. Cvetič, I. Garcia Etxebarria and J. Halverson, Three Looks at Instantons in F-theory New Insights from Anomaly Inflow, String Junctions and Heterotic Duality, JHEP 11 (2011) 101 [arXiv:1107.2388] [INSPIRE].
- [17] A. Grassi, J. Halverson and J.L. Shaneson, Matter From Geometry Without Resolution, JHEP 10 (2013) 205 [arXiv:1306.1832] [INSPIRE].
- [18] A. Grassi, J. Halverson and J.L. Shaneson, Non-Abelian Gauge Symmetry and the Higgs Mechanism in F-theory, Commun. Math. Phys. 336 (2015) 1231 [arXiv:1402.5962] [INSPIRE].

- [19] A. Grassi, J. Halverson, J. Shaneson and W. Taylor, Non-Higgsable QCD and the Standard Model Spectrum in F-theory, JHEP 01 (2015) 086 [arXiv:1409.8295] [INSPIRE].
- [20] A. Grassi, J. Halverson and J.L. Shaneson, Geometry and Topology of String Junctions, arXiv:1410.6817 [INSPIRE].
- [21] A. Grassi, J. Halverson, F. Ruehle and J.L. Shaneson, Dualities of deformed $\mathcal{N}=2$ SCFTs from link monodromy on D3-brane states, JHEP **09** (2017) 135 [arXiv:1611.01154] [INSPIRE].
- [22] A. Collinucci and R. Savelli, F-theory on singular spaces, JHEP **09** (2015) 100 [arXiv:1410.4867] [INSPIRE].
- [23] A. Grassi, J. Halverson, C. Long, J.L. Shaneson and J. Tian, Non-simply-laced Symmetry Algebras in F-theory on Singular Spaces, JHEP 09 (2018) 129 [arXiv:1805.06949] [INSPIRE].
- [24] W. Taylor and Y.-N. Wang, A Monte Carlo exploration of threefold base geometries for 4d F-theory vacua, JHEP 01 (2016) 137 [arXiv:1510.04978] [INSPIRE].
- [25] J. Halverson, C. Long and B. Sung, Algorithmic universality in F-theory compactifications, Phys. Rev. D **96** (2017) 126006 [arXiv:1706.02299] [INSPIRE].
- [26] P. Arras, A. Grassi and T. Weigand, Terminal Singularities, Milnor Numbers, and Matter in F-theory, J. Geom. Phys. 123 (2018) 71 [arXiv:1612.05646] [INSPIRE].
- [27] J.D. Velez and C.A. Cadavid, Normal factorization in sl(2, z) and the confluence of singular fibers in elliptic fibrations, arXiv:0802.0005.
- [28] A. Grassi, J. Halverson, C. Long, J.L. Shaneson, B. Sung and J. Tian, to appear.
- [29] V.V. Prasolov, Elements of combinatorial and differential topology, Graduate Studies in Mathematics. Vol. 74, American Mathematical Society, Providence, U.S.A. (2006).
- [30] J. Halverson, Strong Coupling in F-theory and Geometrically Non-Higgsable Seven-branes, Nucl. Phys. B 919 (2017) 267 [arXiv:1603.01639] [INSPIRE].
- [31] A. Grassi and D.R. Morrison, Anomalies and the Euler characteristic of elliptic Calabi-Yau threefolds, Commun. Num. Theor. Phys. 6 (2012) 51 [arXiv:1109.0042] [INSPIRE].
- [32] A. Grassi and T. Weigand, On topological invariants of algebraic threefolds with (Q-factorial) singularities, arXiv:1804.02424 [INSPIRE].
- [33] S.H. Katz and C. Vafa, *Matter from geometry*, *Nucl. Phys. B* **497** (1997) 146 [hep-th/9606086] [INSPIRE].